THE USE OF ACOUSTICS FOR THE WOOD QUALITY

ASSESSMENT OF STANDING *P. TAEDA* TREES

by

JERRY M. MAHON, JR.

(Under the Direction of Richard F. Daniels)

ABSTRACT

One method of evaluating potential wood product performance is the use of acoustic tools for identifying trees with high stiffness. Acoustic velocities for 100 standing loblolly pine (*Pinus taeda*) trees, obtained with the transmitting and receiving probes placed on the same-face and opposite-faces, were compared using FAKOPP's TreeSonic. Significant differences in velocity between the two methods were found. Variation in velocities from hit-to-hit was 62% less using the opposite-face method compared to the same-face method. A felled tree acoustic device, Fibre-Gen's HM200, was used to evaluate the 6 potential flight paths. Standing tree acoustic velocities were calculated for all 6 flights paths for 79 loblolly trees, in addition to felled tree acoustic velocities. There was no one particular hypothesized flight path that predicted felled tree acoustics overwhelmingly better than any other flight path. It was found that acoustic velocity, both in standing and felled trees increased with age.

INDEX WORDS: Acoustic velocity, analysis of covariance, FAKOPP, Fibre-Gen, HM200, loblolly pine, time of flight, TreeSonic

THE USE OF ACOUSTICS FOR THE WOOD QUALITY

ASSESSMENT OF STANDING *P. TAEDA* TREES

by

JERRY M. MAHON, JR.

BSFR, The University of Georgia, 2005

A Thesis Submitted to the Graduate Faculty of The University of Georgia in Partial Fulfillment

of the Requirements for the Degree

MASTER OF SCIENCE

ATHENS, GEORGIA

2007

THE USE OF ACOUSTICS FOR THE WOOD QUALITY

ASSESSMENT OF STANDING *P. TAEDA* TREES

by

JERRY M. MAHON, JR

Major Professor: Richard F. Daniels

Committee: Laurence R. Schimleck
Thomas G. Harris

Electronic Version Approved:

Maureen Grasso
Dean of the Graduate School
The University of Georgia
December 2007

DEDICATION

This thesis is dedicated to my grandfather, Robert Lee Mahon, who died May 19, 2006, one year into my graduate work. He was an affectionate and worshipful husband; a dedicated father of 3; a supportive, generous, and loving grandfather of 4; a man of great character and integrity; an avid Atlanta Braves fan; a veteran of World War II; a great American; a man truly committed to Christ Jesus; and my hero. This is for you Pap-paw.

ACKNOWLEDGEMENTS

I would first like to thank my major professor, Dr. Dick Daniels, for making this chapter in my life possible. Thank you for the opportunity to work under you, although I did not deserve it. This has been a great time in my life. Thank you for your graciousness and generosity over the last few years.

I would like to thank my committee for the countless hours of work put into this thesis. Thanks to Dr. Laurie Schimleck for his comradery, hard work, insightfulness, and motivation. Thanks to Tom Harris for his patience and understanding. Thanks to Alex Clark, of the USDA Forest Service – my boss, confidant, and fellow Bulldog fan for being with me from the beginning.

Lewis Jordan – this thing would have been impossible without you. Thanks for all your help – it means a whole lot to me. I consider myself lucky to have had you to work with on this research. Ben Hornsby – I'm so glad that we go to share the grad school triumphs and struggles together. Lewis and Ben, your friendship means a whole lot more than the forestry discipline, field-work in hellaciously hot locations, chainsawing, increment boring, and statistics. People will forget about all the research we did together in years to come, but you will both be lifelong friends, and that is far more important to me.

Thanks to the esteemed Dean Mike Clutter for all his words of encouragement, leadership, and friendship the last few years. Thanks for investing in me.

I could not thank enough the people who sacrificed their precious time away from their normal, fun, and enjoyable lives; friends, families, girlfriends, and fiancés for the sake of this research: Christian Mora, Jackson Wyss, Coby Smith, Patrick Work, Drew McCarley, and Christy Stegal. The Log and Lumber crew once again showed their superior workmanship. I can't fail to mention Edward Andrews. You have kept me laughing the last 5 years.

I must thank my friends in Athens who have stuck with me through thick and thin the last few years of my life: Dominique Elkins, Joe O'Brien, Mac Callaham, Matt West, and Keri Whayne.

I would be amiss if I did not thank my best friends – my "inner circle": Tim Carley, Josh Doster, Ricky MacDonald, Kyle Nelson, and Ryan "Chavez" Meeks. Thanks for the prayers and all the fun we've had together. Hunting and fishing would be boring without y'all – so would life.

I could not say thanks enough to my family. To Coach Jerry M. Mahon, Sr., my namesake, his beautiful wife and my mother Olivia, and my amazing brother David – your support, encouragement, blessings, edification, and prayers have meant the world to me. I love you all dearly.

Finally, I could not have done this without my Lord and Savior Jesus Christ. He is my Stronghold, my Rock, and my Salvation. TO GOD BE THE GLORY!

TABLE OF CONTENTS

LIST OF FIGURES

LIST OF TABLES

CHAPTER 1

INTRODUCTION AND LITERATURE REVIEW

INTRODUCTION AND BACKGROUND

The southeastern United States of America is one of the major producers of forest products in the world. Accounting for only 2% of the world's forested land and 2% of the total timber inventory, the US South which includes 7% of planted land, produces 18% of the world's industrial roundwood, and 25% of the world's pulpwood supply (TimberMart South 2005). On the whole, the US South is responsible for 16% of total wood produced in the world. On the national level, the South is responsible for 58% of the wood produced in the USA (Wear and Greis 2002). This region is also responsible for 80% of the trees planted in the USA (McKeand *et al.* 2003). Economically forestry is very important to this region of the world, but possibly, of greater importance, is how this region's forests are managed for contemporary forest products.

The trend in forestry in the US South is to maximize growth as landowners (private or industrial) want trees they can harvest at a young age to recover planting and management costs. Younger wood is lower in specific gravity (SG) and stiffness, while fast-grown wood has a larger diameter core of juvenile wood (Clark and Daniels 2002). Wood procurement managers are faced with buying wood that is potentially lower in quality than that from the past, due to lower specific gravity, lower stiffness, and larger juvenile cores. Where and how they will procure wood that will adequately supply their mills, not just in quantity, but with the desired wood quality presents an interesting dilemma.

To overcome this dilemma, there is an ever increasing need to identify stands with desirable wood quality particularly as stands in the US South become more intensively managed. In addition to wood density or specific gravity, wood stiffness, measured by the modulus of elasticity (MOE), is the most important wood quality trait of interest to southern pine forest products manufacturers. Many researchers are presently investigating the implementation of acoustic tools assess wood stiffness of both standing and felled trees.

WOOD QUALITY DEFINITION

Briggs and Smith (1986) define wood quality as "a measure of the aptness of wood for a given use." Haygreen and Bower (1996) state a specific wood quality definition can be "elusive" because wood quality properties for one product might differ from another. These properties might include: density, uniformity of growth rings, percent of knot-free wood, proportion of latewood, or cellulose yield, to name a few. Larson (1969) considers wood quality a "concept" because important wood properties are arbitrarily classified.

WOOD QUALITY'S TRAITS

The juvenile core is wood that is produced by young cambium, and it has wood quality properties that are undesirable compared to mature wood (Neale *et al.* 2002). Over the past 50 years, a larger juvenile core has developed with decreased rotation lengths (Clark *et al.* 2004; Fox *et al.* 2004). The characteristics of juvenile wood that are unfavorable include: lower specific gravity, lower cellulose content, increased hemicellulose and lignin contents, thinner cell walls, higher microfibril angles, shorter tracheids, and greater amounts of compression wood (Haygreen and Bower 1996). Jordan *et al.* (2007) showed that the length of juvenile core production increased from the southern end of the range of loblolly pine (*Pinus taeda* L.) north and from east to west.

Specific gravity is a key wood property. It is the ratio of the density of a material (here wood) in relation to the density of water (Haygreen and Bower 1996). It is highly correlated with wood quality (Clark and Daniels 2002). Specific gravity is also highly correlated with strength (modulus of rupture or MOR) and stiffness (modulus of elasticity or MOE) in solid forest products and pulp yields (Clark *et al.* 2004).

Stiffness is the resistance to bending. In a wood sample, this is the linear relationship between the amount of stress and resulting strain (Lasserre *et al.* 2007, Haygreen and Bower 1996). Stiffness increases with increased specific gravity and decreased microfibril angle. While strength properties in all growing regions of loblolly pine meet the desired strength thresholds established for southern pine lumber, stiffness properties vary. Stiffness for lumber cut form young timber can approach the minimum standard MOE of 1.6 million PSI. Because specific gravity changes throughout the range of loblolly pine, stiffness varies by physiographic region and can fall below acceptable levels (Jordan *et al.* 2007; Clark and Daniels 2002).

Studies have shown that wood grown in the South Atlantic Coastal and Gulf Coastal Plain can obtain the stiffness properties to make number 2 grade lumber by the age of 15, while in other physiographic regions, it can be as long as 25 years or more (especially northern and western) to produce the same grade lumber. Due to the inconsistency among growing regions, forest managers and wood buyers may have legitimate concerns with stiffness values solid wood products.

Acoustics have become a popular way to estimate stiffness in standing or felled trees with simple, compact, and easy to operate devices (Dickson *et al.* 2004). Stiffness can be estimated by the velocity that a sound wave passes through wood by the equation: $E=pv^2$, where E is the modulus or elasticity, p is the green density of the wood in kg/m^3 and v is velocity in m/s (Chauhan *et al.* 2005, Chauhan and Walker 2006, Lasserre *et al.* 2007). Many researchers have employed these devices to measure wood properties (Ross and Pellegrin 1994; Ross *et al.* 1999; Lindstrom *et al.* 2002; Wang *et al.* 2002, 2004; Lasserre *et al.* 2007).

STANDING TREE ACOUSTICS

Acoustic tools have the potential for providing a rapid, non-destructive method for identifying trees with high stiffness or modulus of elasticity (MOE), and are increasingly being used in the forest industry (Lindstrom *et al.* 2002; Matheson *et al.* 2002; Wang *et al.* 2001, 2007; Grabianowski *et al.* 2006; Toulmin and Raymond 2007). These devices were originally developed to detect decay in trees. There are several acoustic devices employed on standing trees: Fibre-Gen's ST300, FAKOPP's TreeSonic and 2D Timer, TREETAP, and a variety of oscilloscope-based devices.

The devices consist of transmitting and receiving probes. Both are hammered into a tree, with a specified distance between the probes. The transmitting probe is struck with a hammer, inducing a stress wave that passes through the wood to the receiving probe (Lasserre *et al.* 2007). Either a time of flight, which is the time taken for the stress wave to go from the transmitting probe to the receiving probe, or a velocity is displayed in either metric (m/s) or English (ft/s) units. Currently, the most popular acoustic devices for testing standing trees provide time of flight (TOF) and/or acoustic resonance measurements (Lindstrom *et al.* 2002; Grabianowski 2003).

The advantage of using a standing tree acoustic device rather than a felled tree acoustic device is that the tree does not have to be fallen, making it truly non-destructive (Andrews 2000, 2004; Hsu 2004). The limitation of standing tree acoustics is that it measures velocity (or MOE) only in the outerwood rather than through the cross-section of the stem (including the juvenile core) velocity (or MOE) (Andrews 2000; Wang *et al.* 2002; Gorman *et al.* 2003; Hsu 2004).

In the current literature, there are two general methods for measuring acoustic velocity on standing trees: *i*) measurements made with the transmitting and receiving probes are placed on the same-face of the tree at some pre-specified distance, usually about 1 m (Lindstrom *et al.* 2002; Wang *et al.* 2001; Grabianowski *et al.* 2006); and *ii*) measurements made with the transmitting and receiving probes are placed on opposite-faces of the tree at some pre-specified distance, around 1 m (Matheson *et al.* 2002; Joe *et al.* 2004) (Fig. 1). Once velocities have been recorded, researchers have then attempted to correlate standing tree stress wave determined TOF, velocity, or MOE values with observed averaged machine graded MOE from cut boards, green density, or tree characteristics such as DBH.

A component of this research will be to investigate differences between the same face and opposite face methods. It is important for forest managers or procurement foresters to understand how to use the standing tree device.

FELLED TREE ACOUSTICS

There are a variety of acoustic devices that can be used on felled trees and bucked logs. These include: SWAT, WoodSpec, Hitman, and Fibre-Gen's Director HM200. These devices use resonance sound waves as opposed the stress waves used in the standing tree devices (Carter et. al. 2005c).

The HM200, the device we will be investigating in this research, is used by one striking a clear face of a log or felled tree with a hammer. This produces a stress wave that bounces back and forth the length of the log a few hundred times per second. Figure 1.1 shows the flight path of the stress wave induced by the HM200 on a bucked log. Software in the HM200 processes the stress wave's signal and gives a velocity either in metric or English units (Carter *et al.* 2005a). Figure 1.2 shows a screen-shot from the HM200's software where the resonance wave behavior can be seen graphically.

The log velocity is calculated "based on the first harmonic or more using one of its overtones" and the length of the log, which is an input into the device (Chauhan and Walker 2006). Lasserre *et al.* (2007) adds the velocity can be calculated by the following equation: $V=2lfn/n$, where V is the log velocity, l is the log length, f is the resonance frequency, and n is the nth harmonic.

Felled tree velocity has been shown to be more accurate than the time of flight method (Andrews 2000, 2002). This could be attributed to the resonance wave passing through clear wood rather than accommodating branches and bark, like the TOF tools (Lasserre *et al.* 2007). Resonance devices also use a greater distance to average over. Considering the resonance nature (bouncing back and forth many times), this provides for a stabilizing velocity average. While seemingly more accurate, felled tree acoustic methods are destructive.

LITERATURE CITED

Andrews, M. 2000. Where are we with sonics? In: Workshop 2000. Capturing the Benefits of forestry Research: Putting Ideas to Work. Wood Technology Research Centre, University of Canterbury pp. 57-61.

Andrews, M. 2002. Wood quality measurement – son et lumiere. N. Z. J. For. 47:19-21.

Briggs, D.G., and Smith, W.R. 1986. Effects of silvicultural practices on wood properties of conifers – A review. In Douglas-fir: Stand management for the future, C. Oliver, D. Hanley, and J. Johnson, eds. Seattle: Univ. of Washington Press.

Carter, P., Briggs, D., Ross, R.J., and Wang, X. 2005a. Acoustic testing to enhance western forest values and meet customer wood quality needs Productivity of western forests: a forest products focus. Portland, OR : U.S. Dept. of Agriculture, Forest Service, Pacific Northwest Research Station. General technical report PNW ; GTR-642.

Carter, P., Ross, R., and Wang, X. 2005b. Characterizing Softwood Lumber Prior to Processing: New Tools and Results. 59th Forest Products Society International Convention, Québec City, Québec, Canada, 19-22 June, 2005.

Carter, P., Wang, X., Ross, R.J., and Briggs, D. 2005c. NDE of logs and standing trees using new acoustic tools – Technical application and result. Proceedings of the 14th International Symposium on Nondestructive Testing of Wood, May 2-4, 2005, University of Applied Sciences, Eberswalde, Germany. Aachen, Germany: Shaker Verlag, 2005. p.161- 169.

Chauhan, S.S., Entwistle, K.M., and Walker, J.C.F. 2005. Differences in acoustic velocity by resonance and transit-time methods in an anisotropic laminated wood medium. Holzforschung 59:428-434.

Chauhan, S.S., and Walker, J.C.F. 2006. Variations in acoustic velocity and density with age, and their interrelationships in radiata pine. For. Ecol. Manage. 229:388-394.

Clark III, A., and Daniels R.F. 2002. Modeling the effect of physiographic region on wood properties of planted loblolly pine in southeastern United States. Fourth workshop, IUFRO. S5.01.045. Harrison Hot Springs, B.C., CA. Sept 8-14.

Clark III, A., Borders, B.E., and Daniels R.F. 2004. Impact of vegetation control and annual fertilization on properties of loblolly pine wood at age 12. For. Prod. J. 54(12):90-96.

Dickson, R.L., Joe, B., Johnston, D., Notaras, S., Notaras, B., Austin, S., Ribton-Turner, F., and Harris, P. 2004. Pre-processing prediction of wood quality in peeler logs and saw logs. In: Proceedings of the Wood Quality Conference, Albury, NSW, Australia, August.

Fox, T.R., Jokela, E.J., and Allen, H.L. 2004. The evolution of pine plantation silviculture in the Southeastern United States. Gen. Tech. Rep. SRS 75. Ashville, NC: U.S. Dept of Ag., Forest Service, Southern Research Station. 19pp.

Gorman, T.M., Wagner, F.G., and Wu, S.Y., 2003. Assessment of intensive stress-wave scanning of Douglas-fir trees for predicting lumber modulus of elasticity. In: Beall, F.C. (Ed.), Proceedings of the 13th International Symposium on Nondestructive Testing of Wood, August 19-21, 2002. University of California, Richmond, pp. 143-148.

Grabianowski, M. 2003. Measuring acoustic properties in lumber and trees. MSc Thesis, University of Canterbury, Christchurch, New Zealand.

Grabianowski, M., Manley, B., and Walker, J.C.F. 2006. Acoustic measurements on standing trees, logs, and green lumber. Wood Sci. Technol. 40:205-216.

Haygreen, J.G, and Bower, J.L. 1996. Forest products and wood science: an introduction. Third edition. Iowa State University Press. Ames, Iowa.

Hsu, C.Y. 2004. Radiata pine wood anatomy structure and biophysical properties. PhD Dissertation, University of Canterbury, Christchurch, New Zealand.

Joe, B., Dickson, R., Raymond, C., Ilic, J., and Matheson, C. 2004. Prediction of *Eucalyptus dunnii* and *Pinus radiata* timber stiffness using acoustics. RIRDC Publication No. 04/013.

Jordan, L., Clark III, A., Schimleck, L., Hall, D., and Daniels, R.F. 2007. Regional variation in wood specific gravity of plantation grown loblolly pine in the United States. Can. J. For. Res., *in press.*

Larson, P.R. 1969. Wood Formation and the Concept of Wood Quality. Bulletin No. 74. Yale University, School of Forestry.

Lasserre, J.P., Mason, E.G., and Watt, W.S. 2007. Assessing corewood acoustic velocity and modulus of elasticity with two impact based instruments in 11-year-old trees from a clonal-spacing experiment of *Pinus radiata* D. Don. For. Ecol. Manage. 239:217-221.

Lindstrom, H., Harris, P., and Nakada, R. 2002. Methods for measuring stiffness of young trees. Holz Roh Werkst. 60:165-174.

Matheson, A.C., Dickson, R.L., Spencer, D.J., Joe, B., and Ilic, J. 2002. Acoustic segregation of *Pinus radiata* logs according to stiffness. Ann. For. Sci. 59:471-477.

McKeand, S., Mullin, T., Byram T., and White T. 2003. Deployment of genetically improved loblolly and slash pine in the south. J. For. 100(3):32-37.

Neale, D.B., Sewell M.M., and Brown G.R. 2002. Molecular dissection of the quantitative inheritance of wood property traits in loblolly pine. Ann. For. Sci. 59:595-605.

Ross, R.J., Willits, S.W., Segen, W.V., Black, T., Bradshaw, B.K., and Pellerin, R.F. 1999. A stress wave based approach to NDE of logs for assessing potential veneer quality. Part I. Small-diameter ponderosa pine. For. Prod. J. 49(11):60-62.

Ross, R.R., and Pellegrin, R.F. 2004. Nondestructive testing for assessing wood members in structures: a review. General technical report FPL-GTR-70. Forest Products Laboratory. US Forest Service.

TimberMart South. 2005. Southern Timber Market Trends: August 2005. Frank W. Norris Foundation.

Toulmin, M.J., and Raymond, C.A. 2007. Developing a sampling strategy for measuring acoustic velocity in standing *Pinus radiata* using the treetap time of flight tool. N. Z. J. For. Sci. 37(1):96-111.

Wang, X., Carter, P., Ross, R.J., and Brashaw, B.K. 2007. Acoustic assessment of wood quality of raw forest materials – A path to increased profitability. For. Prod. J. 57(5):6-14.

Wang, X., Ross, R.J., and Carter, P. 2007. Acoustic evaluation of wood quality in standing trees. Part I. Acoustic wave behavior. J. Wood and Fiber Sci. 39(1):28-38.

Wang, X., Ross, R.J., Green, D.W., Brashaw, B.K., Englund, K., and Wolcott, M. 2004. Stress wave sorting for red maple logs for structural quality. Wood Sci. Technol. 37:531-537.

Wang, X., Ross, R.J., Mattson, J.A., Erickson, J.R., Forsman, J.W., Geske, E.A., and Wehr, M.A. 2002. Nondestructive evaluation techniques for assessing modulus of elasticity and stiffness of small-diameter logs. For. Prod. J. 52:79-85.

Wang, X., Ross, R.J., McClellan, M., Barbour, R.J., Erickson, J.R., Forsman, J.W., and McGinnis, G.D. 2001. Nondestructive evaluation of standing trees with a stress wave method. J. Wood and Fiber Sci. 33(4):522-533.

Wear, D.N. and J.G. Greis. 2002. Southern forest resource assessment: summary of findings. J. For. 100(7):6-14.

FIGURES FOR CHAPTER 1

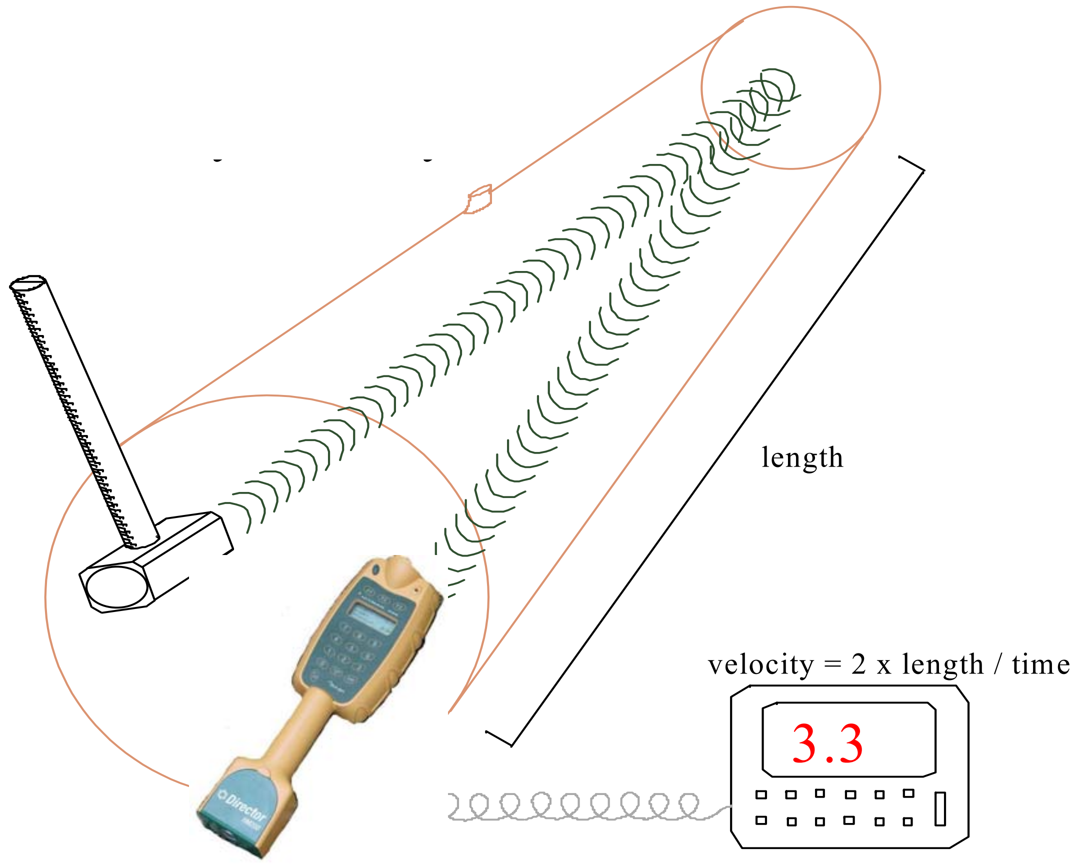

Figure 1.1 HM200 stress wave flight path on a felled log. From Carter *et al.* 2005b.

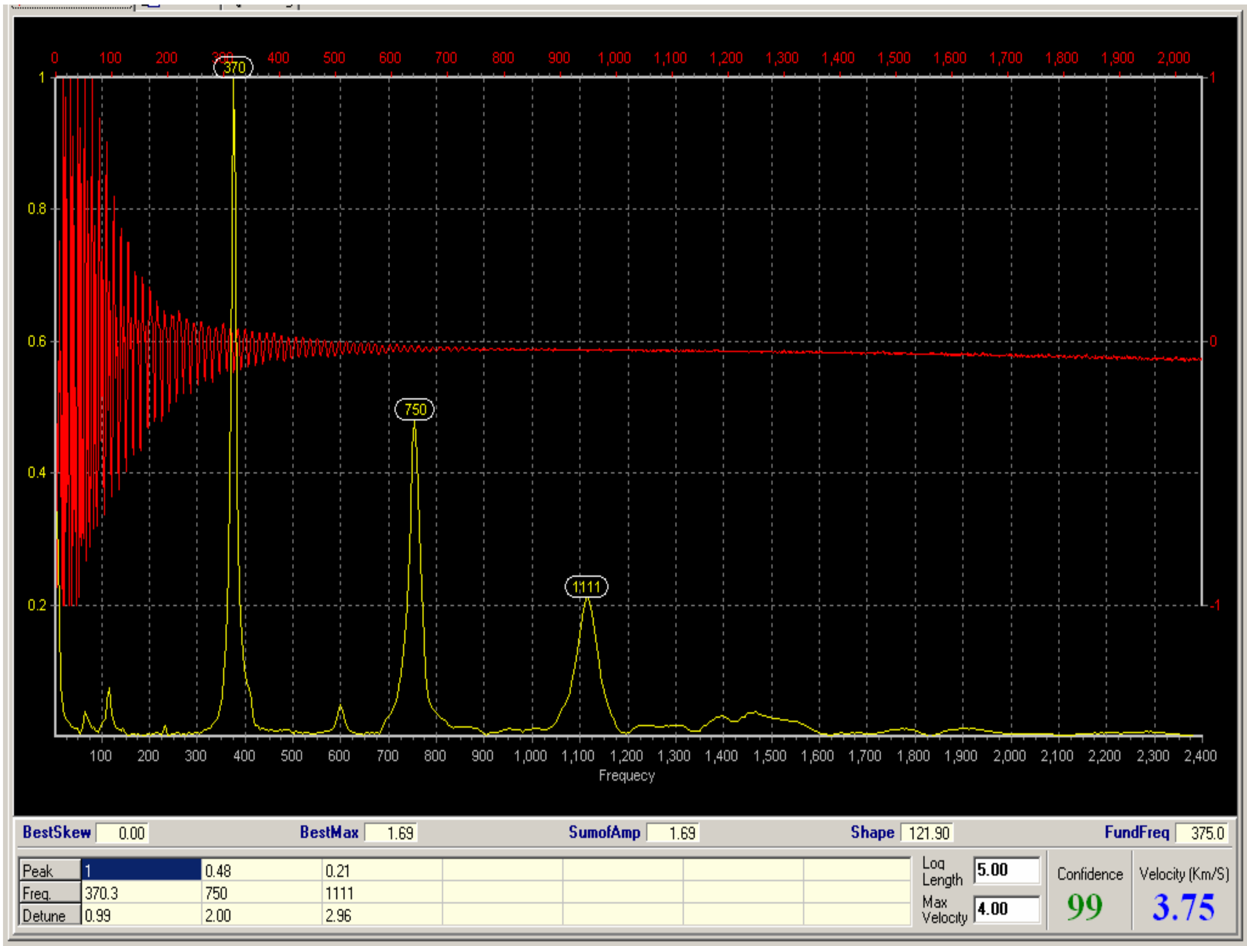

Figure 1.2. Output from HM200 software showing the second harmonic from which the log velocity is calculated. From Carter *et al.* 2005b.

CHAPTER 2

A COMPARISON OF SAMPLING METHODS FOR A STANDING TREE ACOUSTIC DEVICE[1]

[1] Mahon, J.M., Jordan, L., Schimleck, L.R., Clark, A., and Daniels, R.F. To be submitted to *Southern Journal of Applied Forestry*

ABSTRACT

One method of evaluating potential wood product performance is the use of acoustic tools for identifying trees with high stiffness. Acoustic velocities were compared, obtained with the transmitting and receiving probes placed on the same-face and opposite-faces for 100 standing loblolly pine (*Pinus taeda*) trees. Significant differences in velocity between the two methods were found, with velocity determined using the opposite-face method generally dependent on stem diameter, or the amount of wood through which the stress wave must pass. The only opposite face method for which velocity did not vary with diameter at breast height was for an assumed flight path where the stress wave traveled from the transmitting probe around the circumference of the stem in the outerwood and then down longitudinally to the receiving probe. Variation in velocity from hit-to-hit was 62% less using the opposite-face method compared to the same-face method.

KEYWORDS:

Velocity, analysis of covariance, FAKOPP, loblolly pine, mixed-effects, time of flight, TreeSonic

INTRODUCTION

When southern pine dimension lumber is visually graded it is given a grade that has assigned strength and stiffness design values. Young fast growing trees may not have the stiffness required to make No. 2 lumber. Thus, there is an ever increasing need to segregate standing trees or lumber based on certain wood properties or mechanical performance. Early determination of tree stiffness will not only help identify the best end use of the resource, but will also maximize revenue (Matheson *et al.* 2002). Recently acoustic tools have been examined as a rapid, non-destructive method for identifying trees with high stiffness or modulus of elasticity (MOE), and are being used increasingly within the forest industry (Lindstrom *et al.* 2002; Matheson *et al.* 2002; Wang *et al.* 2001, 2007; Grabianowski *et al.* 2006; Toulmin and Raymond 2007).

Acoustic devices generally consist of a transmitting probe which induces a stress wave that travels through the stem and is detected by a receiving probe, located at a known distance from the transmitter. The time it takes for the stress wave to travel from the transmitter to the receiver is recorded, and is known as the time of flight (TOF). For known distance (d), the velocity (v), or the rate of propagation through the material is simply distance divided by TOF (v = d / TOF). If the green density (ρ) of the material is known, the dynamic MOE can then be calculated as ρ multiplied by velocity squared ($MOE = \rho v^2$). Thus, acoustic tools can provide a rapid, nondestructive measure of MOE, the standard for which solid wood products are judged, and are of enormous benefit to the forest products industry.

Numerous authors report strong relationships between stress wave and machine graded MOE (Wang *et al.* 2001; Matheson *et al.* 2002; Joe *et al.* 2004). Wang *et al.* (2001) reports statistically significant relationships between stress wave determined MOE and static MOE of lumber cut from logs with R^2 values ranging from 0.44 to 0.89. Similar results were observed by Matheson *et al.* (2002) when examining the relationship between cut boards and stress wave velocity in logs of radiata pine (*Pinus radiata*) (R = 0.50). Joe *et al.* (2004) when examining the relationship between whole log stress wave velocity and machine graded MOE in *Eucalyptus dunnii*, found correlations of 0.72 and 0.73 for trees 9 and 25-years-old respectively.

These findings verify the utility of acoustics for estimating log and lumber stiffness. However, for practical purposes, evaluation of standing tree stiffness within a plantation prior to harvest is a desirable goal, as it would prevent the present redundancy of sorting high and low stiffness logs after delivery to the mill. If significant relationships can be established between standing tree stress wave determined TOF, velocity, or MOE values, and individual tree characteristics, then this would allow for maximum efficiency in the sorting process.

Matheson *et al.* (2002) found mixed results when correlating standing tree stress wave velocity and lumber cut from logs in radiata pine, reporting correlations of R = 0.33 (control seedlot) and R = 0.01 (orchard lot). Joe *et al.* (2004) also reported significant relationships between standing tree acoustics and machine graded MOE with correlations of R = 0.40 and R = 0.44 in *E. dunnii*. In a recent study, Grabianowski *et al.* (2006) reported standing tree acoustic velocities correlated well with lumber cut both adjacent to the bark and corewood with R^2 values of 0.89 and 0.74, respectively. The significance of diameter at breast height (DBH) on the relationship between acoustic velocity, stress wave determined MOE, and machine graded MOE has also been investigated. Joe *et al.* (2004) found no significant relationships when correlating DBH with acoustic velocity and machine graded MOE values, while Toulmin and Raymond (2007) reported minimal relationships between DBH and acoustic velocities in radiata pine with R^2 values of 0.07, 0.09, and 0.04 for stands aged 10, 15, and 20 years, respectively. Similar findings were reported by Chauhan and Walker (2006) when examining the relationship between acoustic velocity, outerwood density, and DBH in radiata pine stands aged 8, 16, and 25 years. Chauhan and Walker (2006) reported R^2 values of 0.02, 0.07, and 0.18 at 8, 16, and 25 years respectively, when regressing velocity on outerwood density. They also found poor relationships between velocity and DBH with R^2 values of 0.18, 0.06, and 0.14 at 8, 16, and 25 years, respectively.

In the current literature, there are two general methods of measurement for evaluating standing tree acoustics: *i*) the transmitting and receiving probes are placed on the same-face of the tree at some pre-specified distance [generally 1 m] (Lindstrom *et al.* 2002; Wang *et al.* 2001; Grabianowski *et al.* 2006); and *ii*) the transmitting and receiving probes are placed on opposite-faces of the tree at some pre-specified distance [generally 1 m] (Matheson *et al.* 2002; Joe *et al.* 2004) (Figure 2.1). Once velocities have been recorded, researchers have then attempted to correlate standing tree stress wave determined TOF, velocity, or MOE values with observed averaged machine graded MOE from cut boards, green density, or tree characteristics such as DBH.

Matheson *et al.* (2002) conjectures that the induced stress wave "may travel through the heart of the tree (where flight time is expected to be least) or may travel around the tree in the stiffer sapwood (where the flight time is expected to be greatest)", when using the opposite-face method. For TOF, or velocity, determined using the same-face method it is hypothesized that the stress wave travels longitudinally in the wood between the transmitting and receiving probes. However, no research has been done to compare the differences in velocity estimates obtained using the same- and opposite-face methods. This has implications when trying to correlate stress wave determined TOF, velocity, or MOE values with observed averaged machine graded MOE from cut boards, green density, or tree characteristics.

The objective of this work is to examine differences in acoustic velocities using the FAKOPP TreeSonic microsecond timer device when the probes are placed on the same-face and the opposite-face, and to explore possible flight paths for stress waves through standing trees.

MATERIALS AND METHODS

One-hundred loblolly pine trees were sampled from a research plot established in 1989 by the Consortium for Accelerated Pine Production Studies (CAPPS) of the University of Georgia in Clarke County, Georgia USA. The treatment applied to the plot follows that of Borders *et al.* 2004. Herbicides were used to control all herbaceous and woody competing vegetation throughout the life of the plot. Fertilization for the first two growing seasons included 280 kg/ha DAP plus 112 kg/ha KCl in the spring and 56 kg/ha of ammonium nitrate midsummer. In subsequent growing seasons, applications included 168 kg/ha ammonium nitrate early- to mid-spring. At age 10, 336 kg/ha ammonium nitrate plus 140 kg/ha triple super phosphate were applied. At age 11, 560 kg/ha super rainbow (10-10-10) with micronutrients plus 168 kg/ha ammonium nitrate were applied in early spring. At age 12 and forward 336 kg/ha ammonium nitrate were applied in early spring. The trees selected for sampling ranged in diameter at breast height (DBH) from 16.8 – 35.8 cm and average 25.4 cm. Total height of the sample trees ranged from 17.5 – 26.4 m and average 22.1 m.

The FAKOPP TreeSonic device is an acoustic tool designed to study standing trees (Booker and Ridoutt 1997; Lindstrom *et al.* 2002). The FAKOPP TreeSonic is comprised of two probes, a transmitting accelerometer and a receiving accelerometer. For measurements on standing trees it is recommended that the probes are placed 1 m apart. FAKKOP's TreeSonic was used to measure the TOF (m/s) between the transmitting and receiving probes for all 100 trees, from which velocity was calculated. For the same-face method, the probes were positioned 1 m apart and centered on DBH. For the opposite-face method, the transmitting probe was placed 0.5 m above DBH on one face of the tree, the receiving probe was then placed on the opposite face 0.5 m below DBH such that the vertical distance between the transmitting and receiving probes was 1 m (Figure 2.1). To ensure an accurate estimate, both methods were applied on the four cardinal faces of each sample tree, with each face receiving 5 hits, for a total of 20 velocities for each method respectively.

Researchers using the opposite-face method, generally assume that the distance the stress wave travels through the standing tree is 1 m, since this is generally how far apart the probes are placed on the tree (Figure 2.1). This is not an unreasonable assumption using the same-face method, but fails to take into account the amount of wood through which the stress wave must pass when using the opposite-face method, and would lead to underestimated acoustic velocities for larger trees. One alternative is to use a covariate such as DBH to adjust the velocities. However, by calculating the distance between the transmitting and receiving probes using hypothesized flight paths, one can then adjust the velocities accordingly, potentially removing the effect of the amount of wood through which the stress wave passes.

FLIGHT PATHS

We propose six flight paths which the stress wave could take within the stem, leading to six unique acoustic distances and, therefore, velocities (Figure 2.2). These velocities are defined as:

i) Vel_S = the same-face method: assuming the flight path of the stress wave from the transmitting probe travels longitudinally down the wood a distance of 1 m to the receiving probe.

ii) Vel_OU = the unadjusted opposite-face method: assuming a distance of 1 m, the flight path of the stress wave is considered unknown and could travel in any direction through the stem.

iii) Vel_OA = the across adjusted opposite-face method: assuming the flight path from the transmitting probe has an initial direction traveling radially through the center of the stem and down 1 m to the receiving probe.

iv) Vel_OC = the circumference adjusted opposite-face method: assuming the flight path from the transmitting probe has an initial direction traveling circumferentially around the stem in the outerwood and down 1 m to the receiving probe.

v) Vel_OD = the diagonally adjusted opposite-face method: assuming the flight from the transmitting probe travels in a straight line to the receiving probe, passing through the heart of the tree.

vi) Vel_OE = the ellipse adjusted opposite-face method: assuming the flight path from the transmitting probe has an initial direction traveling the shortest distance between the transmitting and receiving probes elliptically through the outerwood across the stem to the receiving probe.

For simplicity, we assumed the 1 m section of the stem between the transmitting and receiving probes was a cylinder, with diameter equal to DBH. The method of calculating the six acoustic velocities are given as:

$$\text{Vel\_S} = 1 / \text{TOF} \quad (1)$$

$$\text{Vel\_OU} = 1 / \text{TOF} \quad (2)$$

$$\text{Vel\_OA} = \left[(\text{DBH}/100) + 1\right] / \text{TOF} \quad (3)$$

$$\text{Vel\_OC} = [(C/2)+1)]/\text{TOF} \quad (4)$$

$$\text{Vel\_OD} = \left(\sqrt{1^2 + (\text{DBH}/100)^2}\right)/\text{TOF} \quad (5)$$

$$\text{Vel\_OE} = \text{D}^* / \text{TOF}, \quad (6)$$

where, $\text{C} = (\text{DBH}\pi)/100$ is the circumference of the stem in meters, $\text{D}^* = \{\pi(\text{a}+\text{b})[1+3\text{h}/(10+\sqrt{4-3\text{h}})]\}/2$, (one-half the circumference of an ellipse), $\text{a} = \sqrt{1^2 + (\text{DBH}/100)^2}$, $\text{b} = (\text{DBH}/100)/2$, and $\text{h} = (\text{a}-\text{b})^2/(\text{a}+\text{b})^2$. D^* was calculated using Ramanujan's second approximation for the circumference of an ellipse.

The distance and corresponding adjusted velocities for each hypothesized flight path can be calculated using the above equations (Table 2.1). The average velocities for each method were found to range from 3092.16 to 4312.25. The distance of the flight path for the Vel_S and Vel_OU methods was held constant at 1 m, and thus averaged 1 m. The average distance of the flight path for Vel_OA, Vel_OC, Vel_OD, and Vel_OE was found to be 1.25, 1.40, 1.03, and 1.11 m, respectively. For the duration of this analysis, we refer to Vel_S as the same-face method, and Vel_OU, Vel_OA, Vel_OC, Vel_OD, Vel_OE, as the opposite-face method.

STATISTICAL ANALYSIS

The experimental design for this study was a randomized complete block design with subsampling. Each sample tree corresponds to a block, the treatment consisting of the method used in calculating velocity (Vel_S, Vel_OU, Vel_OA, Vel_OC, Vel_OD, Vel_OE), and the multiple hits corresponding to the subsample. The general form of this model can be expressed as:

$$y_{ijk} = \mu + \text{M}_i + \text{t}_j + (\text{Mt})_{ij} + e_{ijk}, \quad (7)$$

where, y_{ijk} = the velocity of the *k*th hit of the *j*th tree with the *i*th method $(i = \text{Vel\_S}, \text{Vel\_OU}, \text{Vel\_OA}, \text{Vel\_OC}, \text{Vel\_OD}, \text{Vel\_OE},\ j = 1, \ldots, 100,\ k = 1, \ldots 20)$, μ = the population mean, M_i = the effect of the *i*th method, t_j = the random effect of the *j*th tree, with $\mathrm{t}_j \sim N(0, \sigma^2_{\mathrm{t}})$, $(\mathrm{Mt})_{ij}$ = the random interaction effect between the *i*th method and *j*th tree with $(\mathrm{Mt})_{ij} \sim N(0, \sigma^2_{\mathrm{Mt}})$, and e_{ijk} is residual error with $e_{ijk} \sim N(0, \sigma^2)$.

Although fairly general, equation (7) does not account for the variability in the trees that could not be controlled by the experimental design. In addition to the response variable (velocity), all trees were measured for DBH. An analysis of covariance (ANCOVA) was performed using DBH as a covariate and the full model can be written as:

$$y_{ijk} = \beta_0 + \beta_{0i} + \beta_1 \mathrm{DBH}_{ij} + \beta_{1i} \mathrm{DBH}_{ij} + \mathrm{t}_j + (\mathrm{Mt})_{ij} + e_{ijk}, \quad (8)$$

where, β_0 and β_1 are the population intercept and slope regression coefficients respectively, β_{0i} and β_{1i} are the treatment effect coefficients, and all other variables previously defined. Equation (8) was fit to compare the velocities calculated using the assumed flight paths. The models were fit using the SAS® MIXED procedure, with Satterthwaite's approximation for computing the denominator degrees of freedom for the fixed effects (SAS Institute Inc. 2004).

RESULTS

We fit the full model, equation (8), to test the hypothesis that all slopes are equal to zero; $H_{\mathrm{o}}: \beta_{1\,\text{Vel\_S}} = \beta_{1\,\text{Vel\_OU}} = \beta_{1\,\text{Vel\_OA}} = \beta_{1\,\text{Vel\_OC}} = \beta_{1\,\text{Vel\_OD}} = \beta_{1\,\text{Vel\_OE}} = 0$ vs. $H_{\mathrm{a}}: (\text{not } H_{\mathrm{o}}:)$. The $F_{6,292}$ value and p-value of this test were 75.78 and 0.0001 respectively. We rejected H_{o}, and concluded that the slopes are most likely not all equal to zero. We then tested the hypothesis $H_{\mathrm{o}}: \beta_{1\,\text{Vel\_S}} = \beta_{1\,\text{Vel\_OU}} = \beta_{1\,\text{Vel\_OA}} = \beta_{1\,\text{Vel\_OC}} = \beta_{1\,\text{Vel\_OD}} = \beta_{1\,\text{Vel\_OE}} = \beta$, to determine if a common slope model would be adequate to describe the data. The $F_{5,491}$ value and p-value of this test were 88.90 and 0.0001, respectively. Rejecting H_{o}, we concluded that the slopes of the six methods were not equal, and that each method required its own slope coefficient when DBH was used as a covariate. We then refit equation (8) specifying $e_{ijk} \sim N(0,\sigma_G^2)$, or separate residual variance components for the same-face and opposite-face groups (*G*). Comparing this model versus $e_{ijk} \sim N(0,\sigma^2)$, is a test of $\sigma^2_{\text{Vel\_S}} = \sigma^2_{\text{Vel\_O}\cdot}$, and can be accomplished via a likelihood ratio test which is asymptotically distributed as χ^2_1. The value of the test statistic, or the differences of twice the negative log-likelihoods, between the full and reduced models was 804.4, with a corresponding p-value of 0.0001, suggesting separate residual errors for the same-face and opposite-face methods.

A plot of the estimated regression lines versus DBH for each method is presented in Figure 2.3. Velocities are generally higher for the Vel_S, Vel_OA, and Vel_OC methods compared to the Vel_OE, Vel_OD, and Vel_OU methods, which assumed a longer flight path. Figure 2.3 also indicates that velocities determined using Vel_S and Vel_OC methods do not vary with increasing DBH. The regression coefficients, corresponding standard errors, p-values, and variance components for the final model are presented in Table 2.2. Plots of the residuals from the final model indicated no general trends or outliers. In Table 2.2, the population regression coefficients correspond to $\beta_{0,\text{Vel\_S}}$ and $\beta_{1,\text{Vel\_S}}$, and $\beta_{0,\text{Vel\_O}\cdot}$ and $\beta_{1,\text{Vel\_O}\cdot}$ correspond to deviations from the population parameters. The slope coefficient for Vel_S was not significantly different from zero ($\hat{\beta}_{1,\text{Vel\_S}} = 1.28$, p-value = 0.7842) and suggests that velocity does not depend on DBH when the probes are placed on the same side of the tree. In other words a simple mean model adequately describes velocities for the same-face method.

The p-values for the estimated slope coefficients of the opposite-face method ($\beta_{1,\text{Vel\_O}\cdot}$) given in Table 2.2, correspond to pairwise comparisons to $\beta_{1,\text{Vel\_S}}$. These results suggest that the slope coefficients of the opposite-face method all differ significantly from $\beta_{1,\text{Vel\_S}}$, with the exception of $\beta_{1,\text{Vel\_OC}}$ (Figure 2.3). Further, this finding indicates that velocity calculated assuming a circumferential flight path around the stem and then downwards to the receiving probe, removes the effect of the amount of wood through which the stress wave passes, but Vel_OU, Vel_OA, Vel_OD, and Vel_OE all depend on DBH (Table 2.2 and 2.3). Finally, the similar slope coefficients for the same-face method and the opposite-face method assuming a circumferential flight path suggests that comparing Vel_S to Vel_OC is equivalent to testing the intercepts. The p-value of this test is equivalent to the p-value of the $\hat{\beta}_{0,\text{Vel\_OC}}$ parameter estimate, and was 0.0001, indicating that the estimate of Vel_OC is significantly larger ($\hat{\beta}_{0,\text{Vel\_OC}} = 500.47$) than Vel_S. Table 2.2 also indicates that Vel_OU, Vel_OA, Vel_OD, and Vel_OE all depend on DBH, or the amount of wood through which the stress wave passes. Pairwise comparisons between the opposite-face methods indicate that the slope coefficients all differ significantly from each other, suggesting no similarities among the distance adjusted velocities (Table 2.3).

Figure 2.4 is a plot of observed velocities calculated using the same-face and opposite-face methods, estimated regression lines and corresponding 95 percent confidence intervals. Estimated values of Vel_S are significantly larger compared to Vel_OU, Vel_OD, and Vel_OE across the range of DBH values. This indicates clearly, that these transformations did not adequately account for the amount of wood through which the stress wave passes. Figure 2.4 also shows no significant differences exist between velocities determined using the Vel_S and

Vel_OA methods across the range of DBH values. The estimates of the pairwise slope comparisons versus $\beta_{1,\mathrm{Vel\_S}}$ (Table 2.3) suggest that the order of effectiveness in removing the effect of stem size, from greatest to least is $\hat{\beta}_{1,\mathrm{Vel\_OC}} = 0.39$, $\hat{\beta}_{1,\mathrm{Vel\_OA}} = 12.95$, $\hat{\beta}_{1,\mathrm{Vel\_OE}} = 17.46$, $\hat{\beta}_{1,\mathrm{Vel\_OD}} = 28.55$, $\hat{\beta}_{1,\mathrm{Vel\_OU}} = 34.95$, respectively.

Plots of observed velocities, estimated regression lines and corresponding 95 percent confidence intervals for comparing velocities determined from the opposite-face methods were also examined. These plots indicated that Vel_OC velocities were significantly higher compared to all other opposite-face adjusted velocities. Similarly, velocities from the Vel_OU method were found to be significantly lower compared to all other opposite-face methods, with the exception of the Vel_OD method. Comparing Vel_OU and Vel_OD across the range of DBH values showed no significant difference between these two methods, meaning that within this diameter range, the velocities are equivalent. Comparing Vel_OE to Vel_OU and Vel_OD, suggested no significant differences in smaller DBH trees, but these curves began to diverge with increasing DBH.

The variance components in Table 2.2, indicate that more variation exists between-trees ($\hat{\sigma}_{\mathrm{t}}^2 = 44557$) than among method by tree combinations ($\hat{\sigma}_{\mathrm{Mt}}^2 = 2606.91$). The inclusion of tree-level covariates such as total height, height to base live crown, or other tree-specific characteristics could be incorporated to reduce the between-tree variation. The residual errors for the methods clearly show more variation from hit-to-hit using the same-face method with $\hat{\sigma}_{\mathrm{Vel\_S}}^2 = 42810$ and residual error values of $\hat{\sigma}_{\mathrm{Vel\_O}\cdot}^2 = 16237$ for the opposite-face methods. This suggests that from hit-to-hit, the same-face method was approximately 2.6 times more variable than the opposite-face methods we examined, i.e. from hit-to-hit the opposite face methods were 62% less variable than the same-face method.

DISCUSSION

The results of this analysis suggest significant differences in velocities when the transmitting and receiving probes of an acoustic instrument are placed on the same- or opposite-faces of a standing tree. These findings generally indicate that velocities, determined using the opposite-face method, depend on the amount of wood, or the size of the stem, through which the stress wave must pass. However, velocity does not depend on stem size when using the same-face method. These findings are in general agreement with Chauhan and Walker (2006) and Toulmin and Raymond (2007), who found low relationships between acoustic velocity and DBH.

The acoustic velocities for the opposite-face methods were generally slower than the same-face method (Vel_S), with the exception being Vel_OC. One possible explanation for the higher velocities using the Vel_OC method is that time of flight was held constant even though the Vel_OC method was assumed to have had a longer flight path than the other methods (Table 2.2). An inherent assumption of the Vel_OC method is that the stress wave travels around the stem faster than it does longitudinally, however, Bucur (2006) reports that ultrasonic velocities are much higher (approximately an order of magnitude) in the longitudinal direction (fiber direction) than the radial or tangential direction.

We also found that the variation of velocities from hit-to-hit was 62 % less using the opposite- versus same-face methods. The reason for this finding is unclear, but may potentially be attributed to the physiological formation of the wood through which the stress wave passes through. In addition, whatever the true flight path, it is clear that the wave travels through more material in any of a number of paths when the probes are on opposite sides. This method is apparently quite stable from one event to another. When the probes are on the same side there is only one path and it could be quite different from one event to another.

Several different flight paths for the opposite-face method were investigated in this work, and of those, the Vel_OC method was the only method that removed the effect of stem size, presumably because it includes the circumference of the tree in its determination. However, numerous alternative flight paths are possible, and may provide results similar to the Vel_OC method. For example, given the stress wave travels fastest in high stiffness (mature) wood, another potential path is possible that involves the stress wave traveling from the transmitting probe radially through the mature wood to the juvenile core, around the circumference of the juvenile core, then radially through the mature wood again on the opposite side of the tree, and then down longitudinally to the receiving probe. This potential flight path is a combination of the Vel_OA (across the stem then down) and Vel_OC (circumferentially around the stem in the mature wood then down) methods. The distance traveled assuming this flight path would be larger than those calculated using the Vel_OA (average distance of 1.25 m) method and smaller than those calculated using the Vel_OC method (average distance of 1.40 m). The combination of the Vel_OA and Vel_OC methods could potentially remove the effect of stem size observed with the Vel_OA method. This transformation would also yield lower velocities than those observed using the Vel_OC method, since for fixed time, decreasing the distance traveled will result in a lower velocity.

Researchers who attempt to calculate stress wave determined MOE from acoustic tools and green density may not be accurate in their estimate if the opposite-face method is used and velocities are not adjusted accordingly. If density is held constant, and velocity is not adjusted for the distance the stress wave travels, then dynamic MOE will be underestimated as stem size increases. Similarly, if velocity is unadjusted and a whole-core or average stem density is used, then dynamic MOE will again be underestimated, and attempting to correlate a whole-tree average for machine graded MOE based on cut boards could lead to erroneous results. This may explain the low correlations observed by Matheson *et al.* (2002), when they correlated unadjusted velocity measured on standing trees with a whole-tree average for board stiffness.

CONCLUSIONS

Comparison of acoustic velocities measured using transmitting and receiving probes placed on the same-face and opposite-faces for 100 standing loblolly pine (*Pinus taeda*) trees, showed significant differences in velocity between the two methods. Velocity determined using the opposite-face method generally depending on stem size, or the amount of wood through which the stress wave must pass. For the opposite-face method five possible flight paths were examined and the only opposite face method whose velocities did not vary with diameter at breast height was for an assumed flight path where the stress wave traveled from the transmitting probe around the circumference of the stem in the outerwood and then down longitudinally to the receiving probe. Variation in velocities from hit-to-hit was 62% less using the opposite-face method compared to the same-face method.

LITERATURE CITED

Booker, R., and Ridoutt, B.G. 1997. Stiffness testing of standing trees. FRI Bulletin 202.

Borders, B.E., Will, R.E., Markewitz, D., Clark III, A., Hendrick, R., Teskey, R.O., and Zhang, Y. 2004. Effect of complete competition control and annual fertilization on stem growth and canopy relations for a chronosequence of loblolly pine plantations in the lower coastal plain of Georgia. For. Ecol. Manage. 192:21-37.

Bucur, V. 2006. Acoustics of Wood, 2nd edn. Springer-Verlag, Berlin Heidelberg New York.

Chauhan, S.S., and Walker, J.C.F. 2006. Variations in acoustic velocity and density with age, and their interrelationships in radiata pine. For. Ecol. Manage. 229:388-394.

Grabianowski, M., Manley, B., and Walker, J.C.F. 2006. Acoustic measurements on standing trees, logs, and green lumber. Wood Sci. Technol. 40:205-216.

Joe, B., Dickson, R., Raymond, C., Ilic, J., and Matheson, C. 2004. Prediction of *Eucalyptus dunnii* and *Pinus radiata* timber stiffness using acoustics. RIRDC Publication No. 04/013.

Lindstrom, H., Harris, P., and Nakada, R. 2002. Methods for measuring stiffness of young trees. Holz Roh Werkst. 60:165-174.

Matheson, A.C., Dickson, R.L., Spencer, D.J., Joe, B., and Ilic, J. 2002. Acoustic segregation of *Pinus radiata* logs according to stiffness. Ann. For. Sci. 59:471-477.

SAS Institute Inc. SAS 9.1.3 Help and documentation. Cary, NC: SAS Institute Inc., 2000-2004.

Toulmin, M.J., and Raymond, C.A. 2007. Developing a sampling strategy for measuring acoustic velocity in standing *Pinus radiata* using the treetap time of flight tool. N. Z. J. For. Sci. 37(1):96-111.

Wang, X., Ross, R.J., McClellan, M., Barbour, R.J., Erickson, J.R., Forsman, J.W., and McGinnis, G.D. 2001. Nondestructive evaluation of standing trees with a stress wave method. J. Wood and Fiber Sci. 33(4):522-533.

Wang, X., Ross, R.J., and Carter, P. 2007. Acoustic evaluation of wood quality in standing trees. Part I. Acoustic wave behavior. J. Wood and Fiber Sci. 39(1):28-38.

FIGURES AND TABLES FOR CHAPTER 2

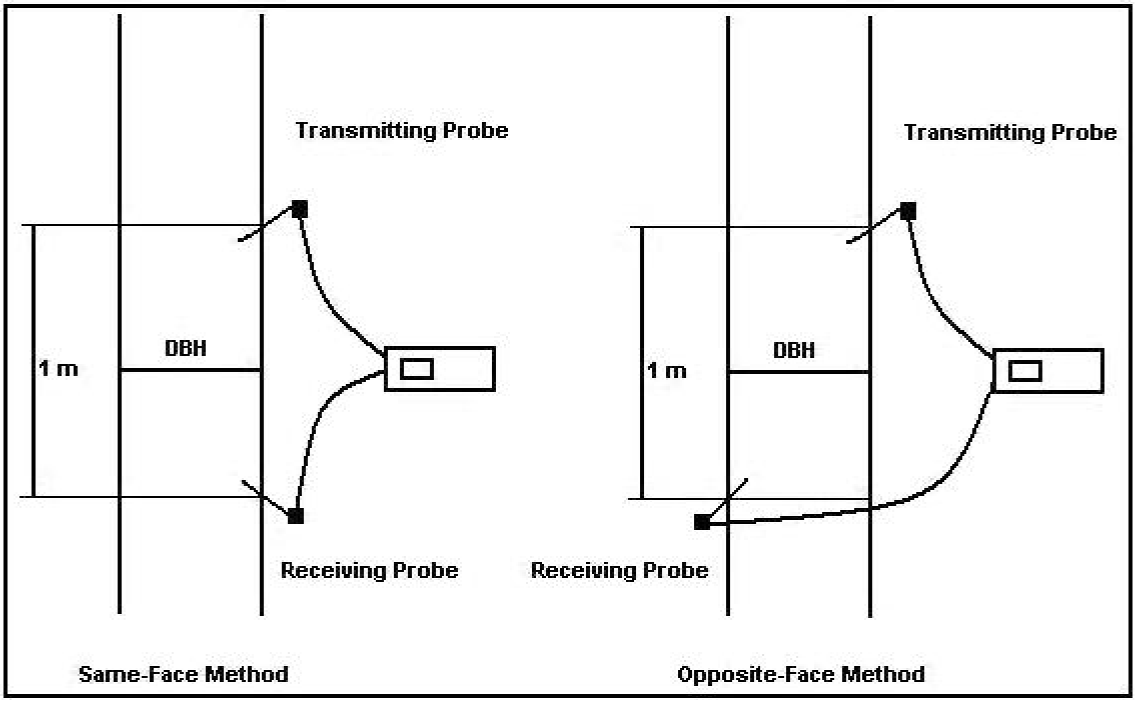

Figure 2.1. Experimental setup to compare same-face and opposite-face methods.

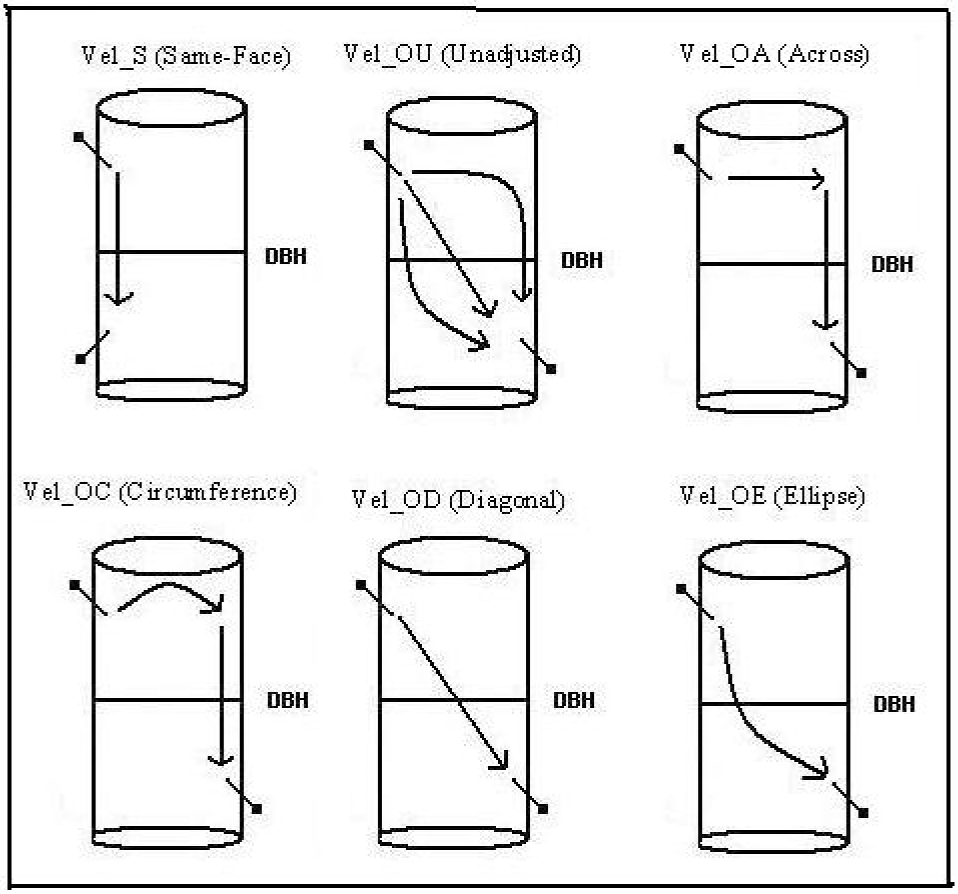

Figure 2.2. Hypothesized stress wave flight paths for the same-face and distance adjusted values.

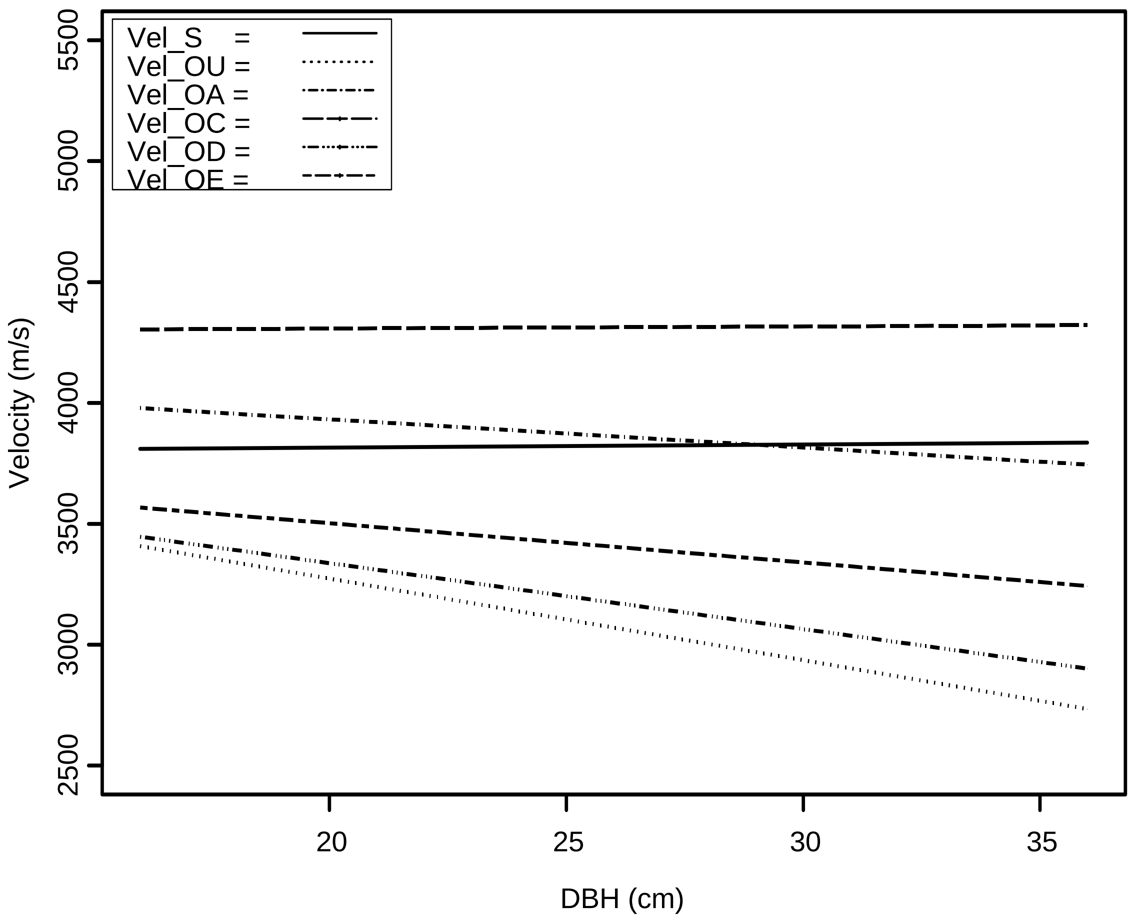

Figure 2.3. Plot of estimated regression lines for comparing same-face and opposite-face determined velocity.

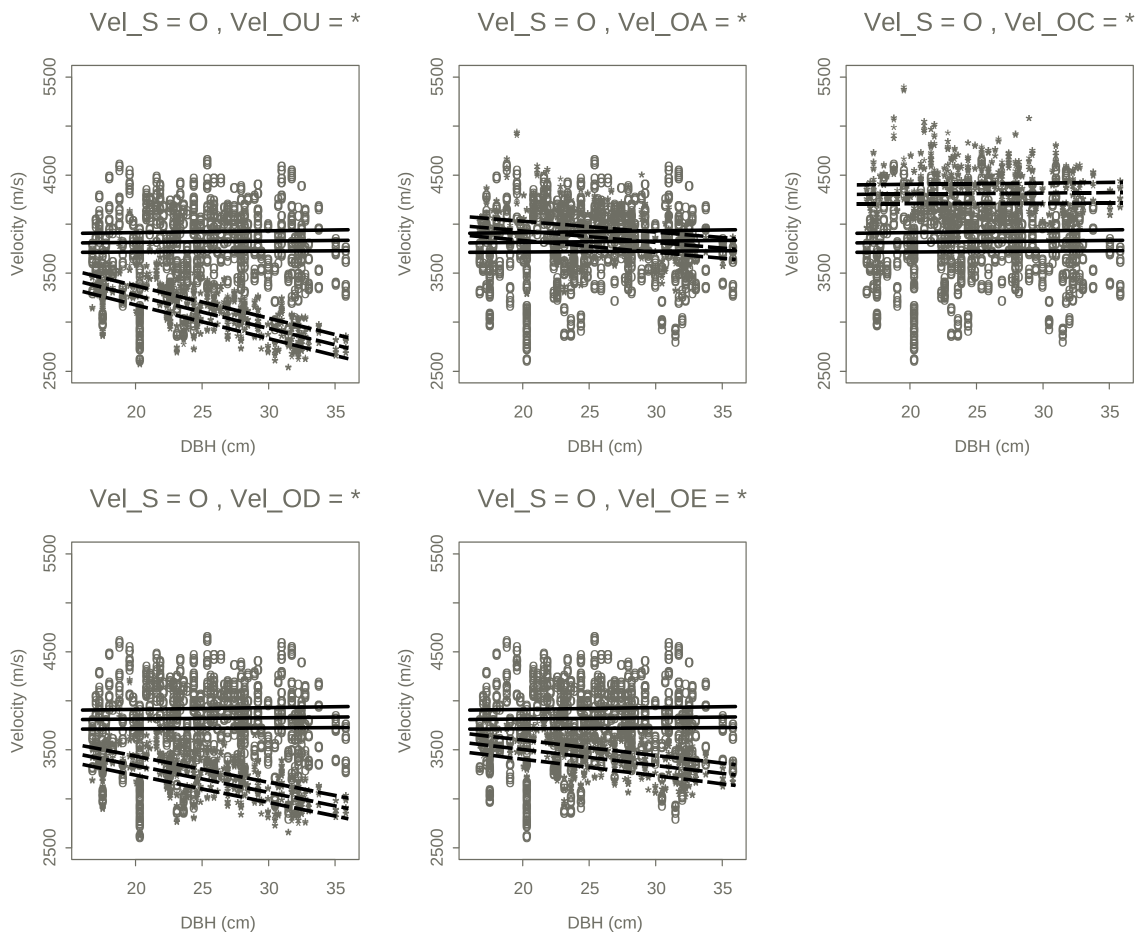

Figure 2.4. Plot of observed velocities, estimated regression lines [O = ———, * = – – – – –] and corresponding 95 percent confidence intervals, for comparing same-face and opposite-face determined velocity.

Table 2.1. Average and range (in parenthesis) of velocities and distances for each hypothesized flight path.

Method	Velocity (m / s)	Distance (m)
Vel_S (Same-Face)	3821.77 (2604.17 – 4651.16)	1.00 (1.00 – 1.00)
Vel_OU (Unadjusted)	3092.16 (2487.56 – 4098.36)	1.00 (1.00 – 1.00)
Vel_OA (Across)	3868.89 (3030.73 – 4899.92)	1.25 (1.17 – 1.36)
Vel_OC (Circumference)	4312.25 (3332.89 – 5357.44)	1.40 (1.26 – 1.56)
Vel_OD (Diagonal)	3191.37 (2570.37 – 4176.01)	1.03 (1.01 – 1.06)
Vel_OE (Elliptical)	3415.32 (2699.26 – 4373.28)	1.11 (1.05 – 1.19)

Table 2.2. Regression coefficients, corresponding standard errors, p-values, and variance components for the final model. Where $\beta_{0,\text{Vel\_S}}$ and $\beta_{1,\text{Vel\_S}}$ correspond to the population level parameters, and $\beta_{0,\text{Vel\_O}\cdot}$ and $\beta_{1,\text{Vel\_O}\cdot}$ correspond to deviations from the population parameters.

Effect	Estimate	Standard Error	DF	t-value	p-value
$\hat{\beta}_{0,\text{Vel\_S}}$	3789.33	120.22	114	31.52	0.0001
$\hat{\beta}_{0,\text{Vel\_OU}}$	156.87	48.93	399	3.21	0.0015
$\hat{\beta}_{0,\text{Vel\_OA}}$	375.61	48.93	399	7.68	0.0001
$\hat{\beta}_{0,\text{Vel\_OC}}$	500.47	48.93	399	10.23	0.0001
$\hat{\beta}_{0,\text{Vel\_OD}}$	93.74	48.93	399	1.92	0.0561
$\hat{\beta}_{0,\text{Vel\_OE}}$	36.42	48.93	399	0.74	0.4571
$\hat{\beta}_{1,\text{Vel\_S}}$	1.28	4.66	114	0.27	0.7842
$\hat{\beta}_{1,\text{Vel\_OU}}$	-34.95	1.89	399	-18.44	0.0001
$\hat{\beta}_{1,\text{Vel\_OA}}$	-12.95	1.89	399	-6.83	0.0001
$\hat{\beta}_{1,\text{Vel\_OC}}$	-0.39	1.89	399	-0.21	0.8356
$\hat{\beta}_{1,\text{Vel\_OD}}$	-28.55	1.89	399	-15.06	0.0001
$\hat{\beta}_{1,\text{Vel\_OE}}$	-17.46	1.89	399	-9.21	0.0001
$\hat{\sigma}^2_{\text{t}} = 44557,\ \hat{\sigma}^2_{\text{Mt}} = 2606.91,\ \hat{\sigma}^2_{\text{Vel\_S}} = 42810,\ \hat{\sigma}^2_{\text{Vel\_O}\cdot} = 16237$					

Table 2.3. Estimates and p-values of pairwise comparisons between the slopes.

Comparison	Estimate	Standard Error	p-value
$\beta_{1,\mathrm{Vel\_S}} - \beta_{1,\mathrm{Vel\_OU}}$	34.95	1.89	0.0001
$\beta_{1,\mathrm{Vel\_S}} - \beta_{1,\mathrm{Vel\_OA}}$	12.95	1.89	0.0001
$\beta_{1,\mathrm{Vel\_S}} - \beta_{1,\mathrm{Vel\_OC}}$	0.39	1.89	0.8356
$\beta_{1,\mathrm{Vel\_S}} - \beta_{1,\mathrm{Vel\_OD}}$	28.55	1.89	0.0001
$\beta_{1,\mathrm{Vel\_S}} - \beta_{1,\mathrm{Vel\_OE}}$	17.46	1.89	0.0001
$\beta_{1,\mathrm{Vel\_OU}} - \beta_{1,\mathrm{Vel\_OA}}$	-21.99	1.73	0.0001
$\beta_{1,\mathrm{Vel\_OU}} - \beta_{1,\mathrm{Vel\_OC}}$	-34.55	1.73	0.0001
$\beta_{1,\mathrm{Vel\_OU}} - \beta_{1,\mathrm{Vel\_OD}}$	-6.40	1.73	0.0003
$\beta_{1,\mathrm{Vel\_OU}} - \beta_{1,\mathrm{Vel\_OE}}$	-17.49	1.73	0.0001
$\beta_{1,\mathrm{Vel\_OA}} - \beta_{1,\mathrm{Vel\_OC}}$	-12.55	1.73	0.0001
$\beta_{1,\mathrm{Vel\_OA}} - \beta_{1,\mathrm{Vel\_OD}}$	15.60	1.73	0.0001
$\beta_{1,\mathrm{Vel\_OA}} - \beta_{1,\mathrm{Vel\_OE}}$	4.51	1.73	0.0099
$\beta_{1,\mathrm{Vel\_OC}} - \beta_{1,\mathrm{Vel\_OD}}$	28.15	1.73	0.0001
$\beta_{1,\mathrm{Vel\_OC}} - \beta_{1,\mathrm{Vel\_OE}}$	17.06	1.73	0.0001
$\beta_{1,\mathrm{Vel\_OD}} - \beta_{1,\mathrm{Vel\_OE}}$	-11.09	1.73	0.0001

CHAPTER 3

ASSESSMENT OF STANDING TREE ACOUSTIC MEASUREMENTS FOR WOOD STIFFNESS COMPARED WITH FELLED TREE ACOUSTIC VELOCITIES

INTRODUCTION

After investigating of how sound waves move through a standing tree using FAKOPP's TreeSonic (Chapter 2), we examined which of the proposed flight path might actually be the most appropriate. Finding the most likely flight path, would support inference on what the TreeSonic's stress wave is actually measuring or the type of wood material it is passing through. If successful, this would give managers a tool for predicting stiffness or other wood properties of interest. As discussed in Chapter 2, when applying and measuring the stress waves on opposite faces of the tree, we hypothesized that the flight path in which the stress wave travels around the stem circumfrentially and down to the receiving probe might best explain the wave path through the tree because it explained the effect of tree size (DBH) on time of flight.. The next step in our investigation is to correlate TreeSonic velocities to wood properties (or a surrogate wood property) that can be measured on a whole-tree, or whole-log, basis.

We chose to compare standing tree acoustic velocities to felled tree acoustics measured using Fibre-Gen's Director HM200 a resonance tool that is used to determine log velocity. Published research has shown that logs having higher velocities have been shown to have stiffer wood (Joe *et al.* 2004; Dickson and Matheson 2004). This sorting tool is widely used in

Australia and New Zealand and is also being investigated for use by several groups in the United States (Dickson and Matheson 2004; Wang *et al.* 2007; Chauhan and Walker 2006).

On a whole stem or cut log, the operator holds the device at one end of the log (usually the larger end which, if required, is cut to provide a clean, flat surface) and striking the end of the log with a hammer. The hammer's blow creates a sound wave that resonates strongly at various frequencies between both ends of the log. Log velocity is calculated "based on the first harmonic or more using one of its overtones" and the distance of the log, which is an input into the device (Chauhan and Walker 2006).

Our objective was to correlate the observed HM200 values to the 6 different proposed flight paths discussed in Chapter 1 and to test which flight path best predicts felled tree acoustic values.

STUDY LOCATIONS

Five stands were identified for this study. They were selected with the aim of providing a wide range of stiffnesses in the first log. Unfortunately, the stands were not of similar ages, growing stock or managed with similar silvicultural practices. The stands were as follows:

Intensively Managed Stand (HF)

Ten trees, 18-years-old, were selected from an intensively managed stand (HF), identical to the study location in the first chapter. Stand history and silvicultural practices are described in Borders *et al.* (2004) and are also described in Chapter 1. The stand was located at Whitehall Forest in Clarke Co., GA (Piedmont physiographic region). Within the stand, 2 replications were established with 5 trees selected per rep. Since there was no variation in TreeSonic times- of-flight (TOF) among the reps, we combined the reps and considered them to be one study location. Trees ranged in diameter at breast height (DBH) from 16.8 – 35.8 cm and averaged 25.4 cm. Total heights of the dominant/co-dominant trees ranged from 17.5 – 26.4 m and averaged 22.1 m.

Natural Stand 1 (N1)

Five trees, approximately 57-years-old, were selected from a natural stand (N1), located at Whitehall Forest in Clarke Co., GA. This old-field site had once been planted with cotton, but was converted to timberland when much of Whitehall Forest was converted to plantations. The stand was established with natural regeneration and had a mix of loblolly, slash, and longleaf pines. The stand received a consistent burning regime of approximately every 3 to 5 years. Trees ranged in diameter at DBH from 25.9 – 36.8 cm and averaged 30.9 cm. Total heights of the dominant/co-dominant trees ranged from 22.5 – 29.4 m and averaged 25.7 m.

Natural Stand 2 (N1)

Five trees, approximately 28-years-old, were selected in a younger natural stand (N2), located at Whitehall Forest in Clarke Co, GA. The stand was once part of the N1 stand, but was clearcut and allowed to regenerate naturally. It also received prescribed burns every 3 to 5 years to control herbaceous and woody competition. Trees ranged in diameter at DBH from 17.0 – 35.6 cm and averaged 26.8 cm. Total heights of the dominant/co-dominant trees ranged from 15.9 – 23.3 m and averaged 19.1 m.

Full-Sibling Stand (IP)

Eighteen trees, 22-years-old, were selected from located at International Paper's Southland Research complex in Bainbridge, GA (Gulf Coastal Plain physiographic region). This stand, an acre in size, was established to test the full-sibling attributes as related to wood quality properties and growth response. As ongoing research dictated, trees had been removed from the stand for testing purposes, thus we consider this stand to be "thinned." Trees ranged in diameter at DBH from 16.8 – 29.7 cm and averaged 23.1 cm. Total heights of the dominant/co-dominant trees ranged from 19.4 – 21.6 m and averaged 20.4 m.

Clonal Stand 1 (AG)

Forty-one trees, 13-years-old, were selected from a clonal stand (AG), located at Mead-Westvaco's Powell Bay research site in Holly Hill, SC (Atlantic Costal Plain physiographic region). These trees had been propagated by rooted cuttings from clones that had been selected for growth traits. The clonal tree exhibited superior growth rates. This stand included 10 replications. At age 7, five of the reps were thinned from 400 trees per acre (TPA) to 250 TPA. We sampled trees from each of the 10 reps, thinned and unthinned, at age 13. We treated the trees in the same manor as we did those of the HF and AG stands – ignoring the fact that some came from a "thinned" rep and not assuming any further information on the parents of the trees. The stand received complete herbaceous and woody competition control throughout the life of the stand to promote growth. Trees ranged in diameter at DBH from 18.0 – 32.3 cm and averaged 23.7 cm. Total heights of the dominant/co-dominant trees ranged from 17.4 – 23.4 m and averaged 21.2 m.

STANDING TREE MEASUREMENTS

Seventy-nine trees were selected from the 5 different stands. Each tree was first tested with the TreeSonic. Velocities from five hits were recorded from each of 2 sides of the tree using the same and opposite faces for a total of 20 hits per tree. For the opposite face method (OFM) the starting and receiving probes were inserted on opposite faces of the tree, with the probes 1 m apart vertically. For the same face method (SFM) the starting and receiving probes were inserted 1 m apart (vertically) on the same face of the tree. Time of flight (TOF) was recorded and velocities calculated for the following 6 flight paths:

Vel_S – SFM where the stress wave travels downwards longitudinally from the starting to the receiving probe.

Vel_OU – OFM where a flight path was not assumed. The distance used was simply the known vertical distance between the starting and receiving probes (1 m), ignoring the tree's diameter.

Vel_OA – OFM where the assumed flight path for the stress wave was assumed to be across the stem's cross-section at the starting probe and down one meter to the receiving probe. The distance was calculated as the diameter of the tree at the upper probe plus 1 meter vertical distance between probes.

Vel_OC – OFM where the flight path for the stress wave was assumed to be half way around the tree's circumference and down to the receiving probe. The distance was calculated as one-half the circumference of the tree at the upper probe plus 1 meter vertical distance between probes.

Vel_OD – OFM where the flight path for the stress wave was assumed to be the diagonal from the starting probe to the receiving probe through the pith of the tree. The distance was assumed to be the hypotenuse of the triangle formed by the 1 meter vertical distance between probes and the tree's diameter.

Vel_OE – OFM where the flight path for the stress wave is assumed to follow a spiral ("barber-pole") path from the starting to the receiving probe, around and down the tree's outer wood sheaths simultaneously. The distance was calculated using Ramanujan's second approximation for the circumference of an ellipse.

Detailed calculations for each of the flight paths can be found in Chapter 2.

FELLED TREE MEASUREMENTS

After the TreeSonic testing was completed, each tree as felled and delimbed. Detailed taper measurements were made up the stem. The tree was then tested using the Fibre-Gen Director HM200. Five sets of HM200 readings were taken:

1.) For the first 3 logs together (0 – 14.6 m);

2.) The first 2 logs together (0 – 9.8 m);

3.) The third log only (9.8 – 14.6 m);

4.) The second log only (4.9 – 9.8 m); and

5.) The first log only (0 – 4.9 m).

As with the TreeSonic velocities, the 5 HM200 velocities were averaged for each portion. Considering the TreeSonic device on the standing tree was used within the first log, we decided to only use the HM200 readings from the first log. Vel_H will be defined as the average stress wave velocity from the first log of a given tree.

STATISTICAL APPROACH

Log velocities using the HM200 have been shown to be highly correlated with wood stiffness or MOE (Joe *et al.* 2004, Dickson and Matheson 2004). In the current study, we use the HM200 velocities as a surrogate for wood stiffness. Our goal is to develop a method to predict wood stiffness from standing tree measurements, i.e. the non-destructive TreeSonic measurements. Therefore, we are interested in the regression of log velocities (Vel_H) on the standing tree velocities obtained with the TreeSonic toward developing predictions for log velocities.

The HM200 and TreeSonic measurements are highly correlated and linear in nature (Figure 3.1) indicating that linear regression methods would provide the means for developing prediction models for HM200 velocities. The use of mixed models is appropriate to analyze the data so that the same random effects from the final model in Chapter 1 could be incorporated here.

Repeated measures could not be used because velocity observations from the standing tree (TreeSonic) could not be matched up with velocity observations from the felled tree (HM200). Considering we took 20 velocity observations using the TreeSonic (10 each method –

opposite and same), it is impossible to "match" these observations to the HM200. Because we could not incorporate repeated measures, a general linear model was used.

For the purposes of this analysis, the mean velocity was taken from the HM200 readings. Essentially, we have 6 different mean velocities for the standing tree, one for each hypothetical flight path. In addition, the mean was taken from the HM200 observations. From this data, we then fit 6 separate models, one for each TreeSonic flight path. The models were as follows:

Vel_H = Vel_TS + Stand + Residual

Where: Vel_H is the response, or the mean velocity from the first log of each tree; Vel_TS is the mean velocity from each of the 6 different flight paths; Stand is the fixed effect of the stands additive response; and residual is the residual error. Essentially, we fix 6 separate models, just replacing "Vel_TS" with the hypothesized flight path being investigated (Vel_OA – Vel_S).

The stands were incorporated into the model as a categorical variable to separate out the effect of the stand, which may include physiographic, site quality, growing stock, stand management and other effects. It is not our intent to be able to predict HM200 velocities within the stand; however it was not appropriate to combine velocities from all five stands without taking into account the differences among them. Considering the stands were 5 different ages, in 3 different physiographic regions, containing different types of growing stock, and receiving drastically different silvicultural treatments, it was necessary to account for the stand as a fixed effect. The "stand" effect then adjusts the intercept of the model for the stand.

SAS® MIXED and GLM procedures were both used to fit these regression equations so comparisons of the different TreeSonic treatments could be made (SAS Institute Inc. 2004). The goal was be to identify the model that had the best overall fit statistics and thus identify which TreeSonic velocity assumption (the standing tree hypothesized flight path) could best predict the HM200 velocity, our surrogate for wood stiffness.

RESULTS AND DISCUSSION

All 6 TreeSonic velocity treatments do well in predicting the HM200 velocity in the first log. Table 3.1 lists the R^2, MSE (mean square errors), and mean absolute residuals for each model. Based on these statistics, the "best" or "most appropriate" standing tree velocity for predicting log velocity is the Vel_OE method, where the stress wave is assumed to follow a spiral path around and down the tree. The model using Vel_OE as the velocity predictor had the highest R^2 (.890).

Whereas the Vel_OE model correlates best with the HM200 data, upon closer inspection, it is apparent that all the TreeSonic velocities correlate quite well. We can simply say that for this sub-population of 79 loblolly pine trees, the Vel_OE method would be the best one. Considering issues with stand age, location, silvicultural treatments, and growing stock, from this data, we can only speculate as to which velocity calculation method works the best.

Results from the models provide trends that are interesting and might be important to forest managers and procurement foresters. As the TreeSonic velocity increases, the HM200 velocity increases as well – a generally linear trend (Figure 3.1). There is a tailing piece toward the upper extreme of the data that does not fall in line with the rest of the data. This group of data points is associated with the N1 stand, the oldest of all the stands.

Comparing the different TreeSonic velocities shows that the apparent regression slope of the plot does not change all that much, but rather is shifted horizontally and vertically on the x-and y-axis, explained by a change in y-intercept. We hypothesized that because TreeSonic velocity values are so different from one distance calculation treatment to another, that they may have led to somewhat different shapes in their relationship to log velocity. This apparently is not the case and is a key reason we see all the different treatment models fitting relatively close to one another.

The plot of predicted HM200 velocities against the observed TreeSonic values (Figure 3.2) reveals some very interesting trends. Predicted HM200 velocity tends to increase with age. We see that the prediction lines are ordered from lowest to highest in general with age. The bottom lines for the AG and HF stands (13 and 18 years old, respectively) are lowest, indicating the lowest predicted velocities for the youngest stands. The IP and N2 prediction lines (22 and 28 years old, respectively) have the next highest predicted HM200 velocity values. Far above any of the other prediction lines is the N1 stand (57 years old). Higher predicted velocities from older stands is consistent with knowledge that wood and tree stiffness increases with age (Dickson *et al.* 1999)

In all 6 different models, we see that N2 and IP lines are not statistically significant from one another and share a common intercept (Tables 3.2-3.7). Separate slopes were first fit, but were seen to be non-significant, which suggests that a common slope is appropriate for all stands.

Even though we N2 stand is older than the IP stand by 6 years, the intercept is still the same for both stands in all 6 models. A potential explanation for the similar predictions in these two stands has to do with the physiographic province in which the stands are located. The N2 stand is in the Piedmont and the IP stand is in the Lower Coastal Plain. We know that trees grown near the coast relative to the Piedmont grow wood that produces more latewood, hence a higher proportion of stiffer wood (Jordan *et al.* 2007). We know that the velocities of sound waves are closely related to the stiffness of the material they pass (Booker and Ridoutt 1997). So if the coastal tree from the IP stand have more latewood wood than the Piedmont N2 stand, even though they are younger, this might be enough to make up for the difference in the ages.

There appears to be a general trend just in TreeSonic velocities with age. TreeSonic velocities were higher in the older stands and lower in the younger stands (Figure 3.3). Considering older trees generally tend to have higher stiffness values than younger trees due to higher proportions of mature wood within the stem, we hypothesize that the HM200 velocities are being regulated by the stiffness of the trees. We do not yet have stiffness data, but we would expect to see higher stiffnesses in older trees relative to the younger ones.

Figure 3.4 plots the predicted HM200 velocities versus the observed HM200 velocities. There appears to be no heterskedacity, and there appears to be no one prediction model that performs better than the others. Figure 3.5 plots the residuals over the predicted values for all 6 models. We see a relatively tight grouping, equally spaced out around 0, with no discernable trends, indicating the regressions predict the HM200 velocities well without apparent bias. The Vel_S plot does appear to have a couple of outliers, in which probably accounts for its higher residual error as seen in Table 3.1.

The statement that no one prediction model appears to do better than the other can be further strengthened by looking at correlations (Tables 3.8-3.10). Table 3.8 shows Pearson's product moments (correlations) for all the data combined. The correlations do not reflect the fixed effect of the stand, which was included in the model explained earlier. Table 3.9 shows the correlations for the data when broken down by stand; Table 3.10 shows the correlations for the data when broken down by physiographic province. The only difference between Tables 3.9 and

3.10 will be the combining of the HF, N1, and N2 stands because they were all in the Piedmont province.

We see that the TreeSonic velocities that best correlate to the HM200 velocities are not consistent. The best correlations between TreeSonic and HM200 velocities vary between the Vel_OA, Vel_OC, and Vel_OE flight paths. It would make a stronger argument for a "true flight path" if one was consistently most highly correlated with the HM200 velocities. However, this does not appear to be the case. With regard to the goal for this chapter, choosing the flight path calculation that best predicts the HM200 velocity, we must conclude that several methods perform well.

CONCLUSIONS

It was our hope was that one particular standing tree TreeSonic velocity calculation method would stand out from the rest in correlating best with the felled tree HM200 velocity. If this had occurred, this might have given us better inference into which TreeSonic velocity might be the "true" velocity, or at least the one that best predicts the HM200. This was not the case. We did find that HM200 velocity tends to increase in age, as does TreeSonic velocity, and presumably stiffness.

While findings were inconclusive, we can still say that from the 79 trees of interest the Vel_OE flight path best predicted felled tree HM200 acoustics. Further we observed that any OFM has a lower variance than the SFM (which agrees with our findings in Chapter 1). From this, we can conclude that when modeling or correlating standing tree acoustics to felled tree acoustics, the OFM is preferred.

FUTURE WORK

Further investigations are needed to validate a proper standing tree velocity calculation. The key, we believe, will be to determine the actual wood stiffness (Modulus of Elasticity – MOE) for these samples and predict actual stiffness from the sonic velocities. And that will be the next step in this research project.

Many new comparisons and correlation can be made using the new stiffness data from the 79 trees. After determining the actual stiffness and density of the trees, we can use the equation $E=pv^2$ and back into a theoretical velocity for each tree after rearranging the terms into the following: $v=[E/p]^{0.5}$. Likewise, we can use the velocity and density to calculate a theoretical stiffness for each tree. We can further evaluate the potential flight paths by comparing the actual and theoretical stiffness and velocity values for each tree.

We have also acquired a new ultra-sonic testing device for small samples of wood, and through this device, acoustic velocities can be calculated on individual static bending samples. Because the static bending samples come from multiple sections within the cross-section of the tree, we can see how stiffness and density affect the acoustic velocities, i.e. for juvenile versus mature wood.

LITERATURE CITED

Booker, R., and Ridoutt, B.G. 1997. Stiffness testing of standing trees. FRI Bulletin 202.

Borders, B.E., Will, R.E., Markewitz, D., Clark III, A., Hendrick, R., Teskey, R.O., Zhang, Y. 2004. Effect of complete competition control and annual fertilization on stem growth and canopy relations for a chronosequence of loblolly pine plantations in the lower coastal plain of Georgia. For. Ecol. Manage. 192:21-37.

Chauhan, S.S., and Walker, J.C.F. 2006. Variations in acoustic velocity and density with age, and their interrelationships in radiata pine. For. Ecol. Manage. 229:388-394.

Dickson, R.L., and Matheson, A.C. 1999. Management intervention points to improve the wood quality of current and future crops. Emerging Technologies for Evaluating Wood Quality for Processing. Forest Industry Engineering Association, Melbourne 2nd December 1999.

Joe, B., Dickson, R., Raymond, C., Ilic, J., and Matheson, C. 2004. Prediction of *Eucalyptus dunnii* and *Pinus radiata* timber stiffness using acoustics. RIRDC Publication No. 04/013.

Jordan, L., Clark III, A., Schimleck, L., Hall, D., and Daniels, R.F. 2007. Regional variation in wood specific gravity of plantation grown loblolly pine in the United States. Can. J. For. Res., *in press.*

SAS Institute Inc. SAS 9.1.3 Help and documentation. Cary, NC: SAS Institute Inc., 2000-2004

Wang, X., Carter, P., Ross, R.J., and Brashaw, B.K. 2007. Acoustic assessment of wood quality of raw forest materials – A path to increased profitability. For. Prod. J. 57(5):6-14.

FIGURES AND TABLES FOR CHAPTER 3

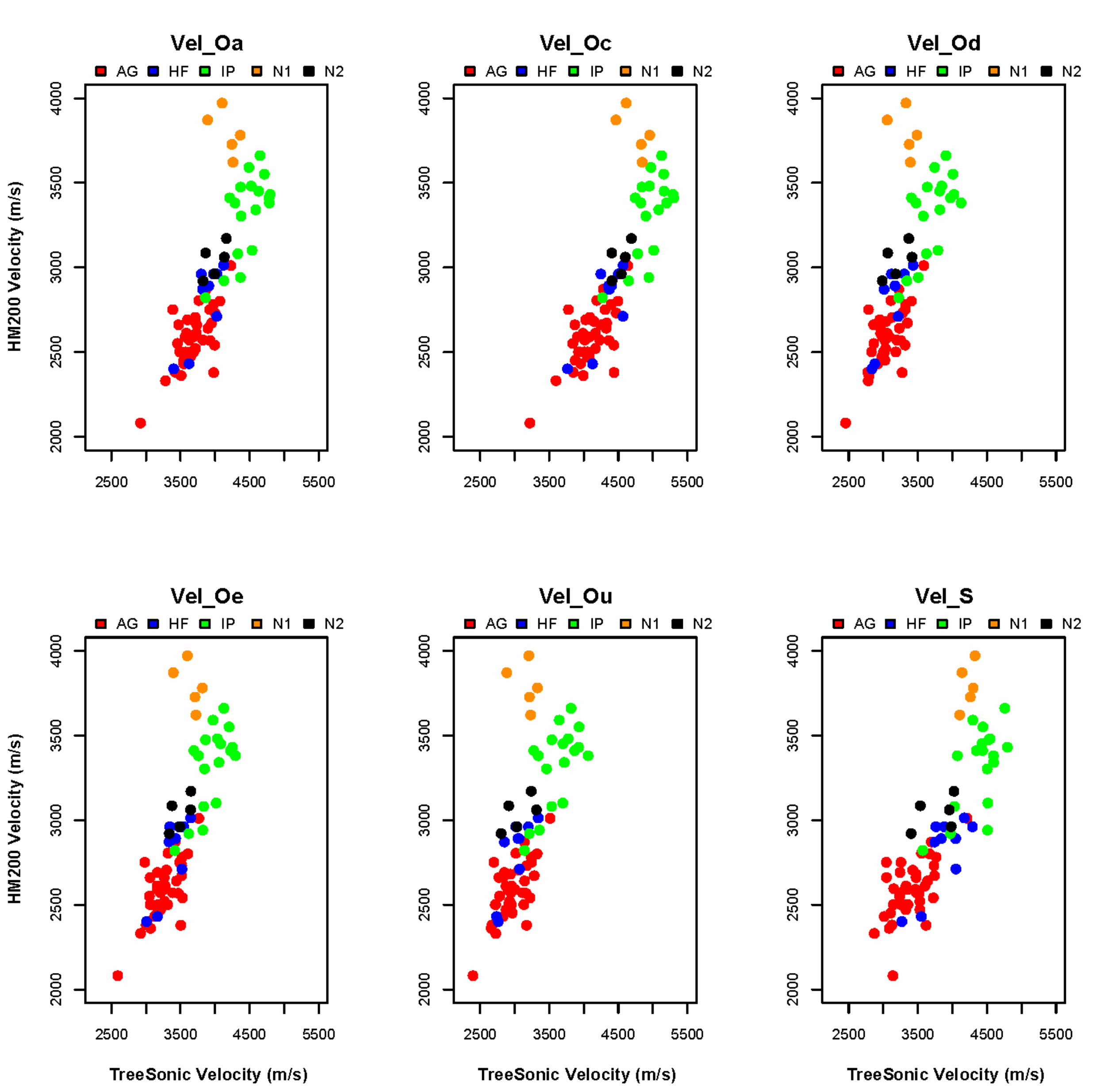

Figure 3.1. Observed HM200 velocity compared to observed TreeSonic velocity by stand.

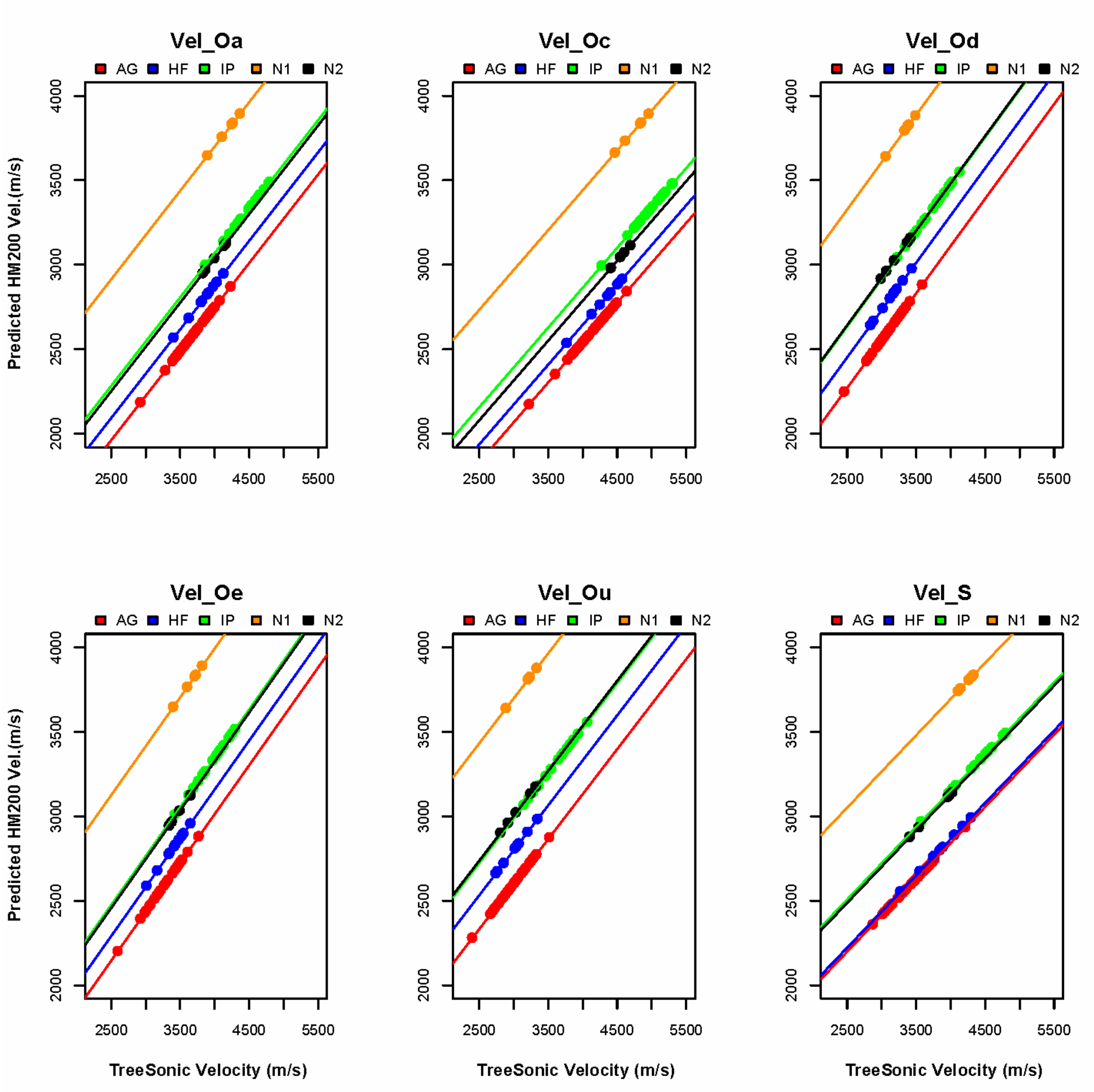

Figure 3.2. Predicted HM200 velocity by observed TreeSonic velocity by stand.

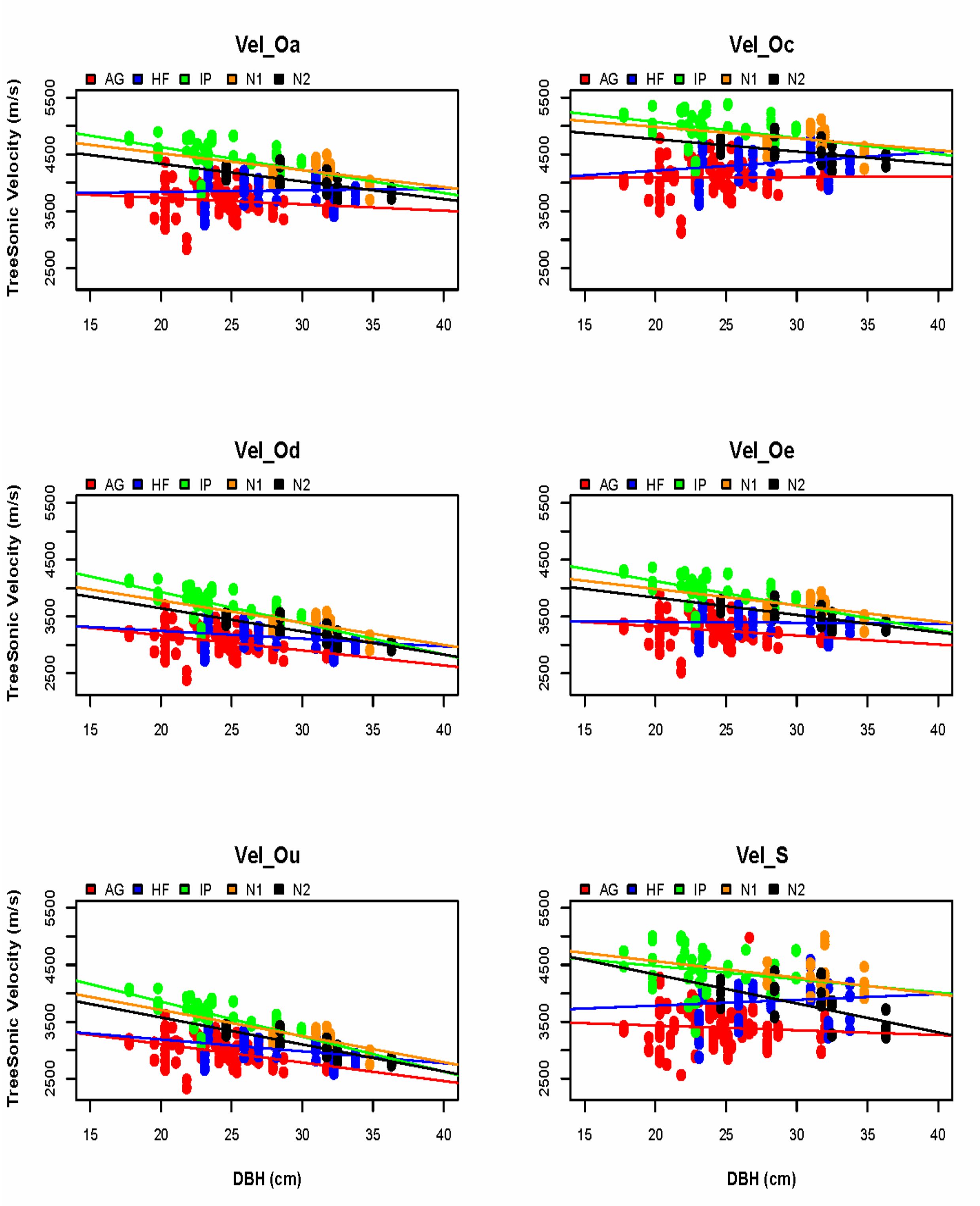

Figure 3.3. Observed TreeSonic velocity by DBH and stand type.

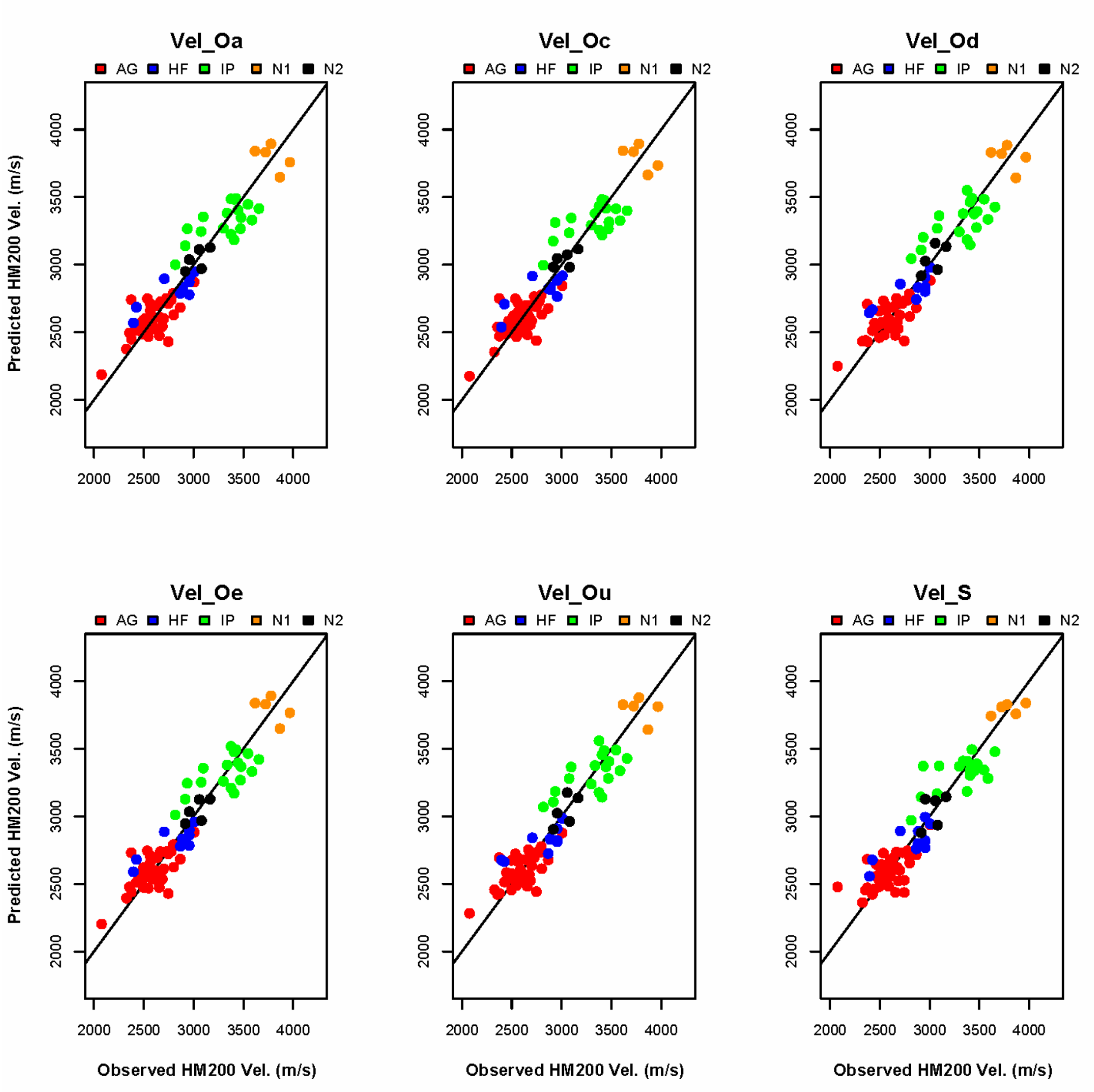

Figure 3.4. Predicted HM200 velocity by observed HM200 velocity by stand.

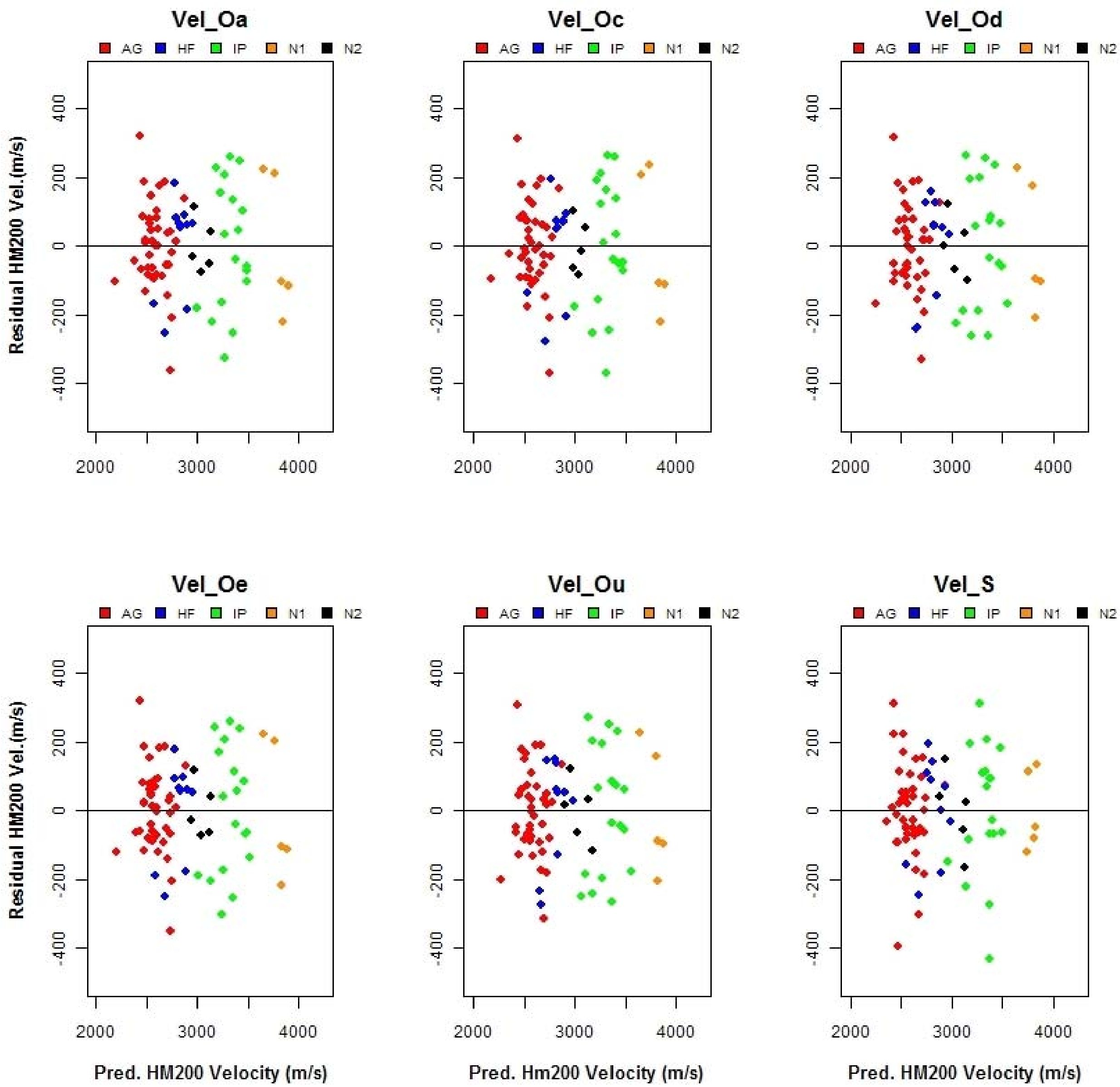

Figure 3.5. Plot of residual HM200 velocity by predicted HM200 velocity.

Table 3.1. Fit statistics for each of the models. The model column shows which TreeSonic velocity value the model was based on.

Model	R^2	MSE	Mean Abs Resid
Vel_OA	0.889	21193	113.78
Vel_OC	0.884	22256	114.34
Vel_OD	0.889	21383	116.11
Vel_OE	0.890	21091	114.56
Vel_OU	0.886	21883	117.47
Vel_S	0.883	22399	113.07

Table 3.2. Regression coefficients, standard errors, and p-values for the **Vel_OA** model. All intercept p-values are differences from the $B_{0,}$ N2 parameter estimate.

Parameter	Estimate	Standard Error	DF	t-value	p-value
$B_{0,}$ AG	650.21	74.72	73	-4.00	0.0002
$B_{0,}$ HF	781.38	83.19	73	-1.98	0.0515
$B_{0,}$ IP	971.79	31.35	73	0.39	0.7003
$B_{0,}$ N1	1602.35	83.07	73	7.12	0.0001
$B_{0,}$ N2	940.44	301.71	73	3.17	0.0023
$B_{1,}$TS	0.5244	0.07	73	7.24	0.0001

Table 3.3. Regression coefficients, standard errors, and p-values for the **Vel_OC** model. All intercept p-values are differences from the $B_{0,}$ N2 parameter estimate.

Parameter	Estimate	Standard Error	DF	t-value	p-value
$B_{0,}$ AG	652.2	76.93	73	-3.22	0.0019
$B_{0,}$ HF	757.17	82.73	73	-1.72	0.0892
$B_{0,}$ IP	977.15	81.00	73	0.96	0.3420
$B_{0,}$ N1	1553.66	95.50	73	6.85	0.0001
$B_{0,}$ N2	899.67	320.9	73	2.80	.00650
$B_{1,}$TS	0.4717	0.07	73	6.81	0.0001

Table 3.4. Regression coefficients, standard errors, and p-values for the **Vel_OD** model. All intercept p-values are differences from the $B_{0,}$ N2 parameter estimate.

Parameter	Estimate	Standard Error	DF	t-value	p-value
$B_{0,}$ AG	871.35	70.24	73	-5.29	0.0001
$B_{0,}$ HF	1052.08	80.29	73	-2.37	0.0203
$B_{0,}$ IP	1235.35	84.02	73	-0.09	0.9311
$B_{0,}$ N1	1927.15	93.00	73	7.36	0.0001
$B_{0,}$ N2	1242.64	259.11	73	4.80	0.0001
$B_{1,}$TS	0.5599	0.08	73	7.16	0.0001

Table 3.5. Regression coefficients, standard errors, and p-values for the **Vel_OE** model. All intercept p-values are differences from the $B_{0,}$ N2 parameter estimate.

Parameter	Estimate	Standard Error	DF	t-value	p-value
$B_{0,}$ AG	699.09	71.53	73	-4.36	0.0001
$B_{0,}$ HF	844.86	80.03	73	-2.08	0.0413
$B_{0,}$ IP	993.08	81.68	73	0.22	0.8262
$B_{0,}$ N1	1679.27	92.61	73	7.21	0.0001
$B_{0,}$ N2	1011.08	285.89	73	3.54	0.0007
$B_{1,}$TS	0.5785	0.08	73	7.28	0.0001

Table 3.6. Regression coefficients, standard errors, and p-values for the **Vel_OU** model. All intercept p-values are differences from the $B_{0,}$ N2 parameter estimate.

Parameter	Estimate	Standard Error	DF	t-value	p-value
$B_{0,}$ AG	1001.13	70.44	73	-5.75	0.0001
$B_{0,}$ HF	1201.16	81.11	73	-2.53	0.0137
$B_{0,}$ IP	1391.64	85.83	73	-0.17	0.8667
$B_{0,}$ N1	2100.66	93.95	73	7.39	.0001
$B_{0,}$ N2	1406.09	243.64	73	5.77	0.0001
$B_{1,}$TS	0.5325	0.08	73	6.96	0.0001

Table 3.7. Regression coefficients, standard errors, and p-values for the **Vel_S** model. All intercept p-values are differences from the $B_{0,}$ N2 parameter estimate.

Parameter	Estimate	Standard Error	DF	t-value	p-value
$B_{0,}$ AG	1128.50	75.02	73	-3.85	0.0002
$B_{0,}$ HF	1152.22	82.13	73	-3.23	0.0019
$B_{0,}$ IP	1436.98	84.83	73	0.23	.8186
$B_{0,}$ N1	1980.63	98.89	73	5.7	.0001
$B_{0,}$ N2	1417.45	249.04	73	5.69	0.0001
$B_{1,}$ TS	0.4283	249.04	73	5.69	0.0001

Table 3.8. Pearson's product moments (correlations) between the TreeSonic velocity and HM200 velocity for all data. Highest correlation is in bold.

Treat	HM200
Vel_OA	0.701
Vel_OC	**0.731**
Vel_OD	0.594
Vel_OE	0.684
Vel_OU	0.520
Vel_S	0.694

Table 3.9. Pearson's product moments (correlations) between the TreeSonic velocity and HM200 velocity for data segregated by stand. Highest correlations are in bold.

HF		N1		N2		IP		AG	
Treat	HM200	Treat	HM200	Treat	HM200	Treat	HM200	Treat	HM200
Vel_OA	0.819	Vel_OA	-0.575	**Vel_OA**	**0.643**	**Vel_OA**	**0.662**	Vel_OA	0.686
Vel_OC	0.775	**Vel_OC**	**-0.666**	Vel_OC	0.613	Vel_OC	0.645	Vel_OC	0.671
Vel_OD	0.820	Vel_OD	-0.424	Vel_OD	0.640	Vel_OD	0.650	Vel_OD	0.677
Vel_OE	**0.827**	Vel_OE	-0.547	Vel_OE	0.636	Vel_OE	0.660	**Vel_OE**	**0.686**
Vel_OU	0.792	Vel_OU	-0.346	Vel_OU	0.641	Vel_OU	0.642	Vel_OU	0.665
Vel_S	0.763	Vel_S	0.550	Vel_S	0.462	Vel_S	0.634	Vel_S	0.597

Table 3.10. Pearson's product moments (correlations) between the TreeSonic velocity and HM200 velocity for data segregated by physiographic region. Highest correlation are in bold.

Piedmont		Atlantic CP		Gulf CP	
Treat	HM200	Treat	HM200	Treat	HM200
Vel_OA	0.701	Vel_OA	0.686	**Vel_OA**	**0.662**
Vel_OC	**0.731**	Vel_OC	0.671	Vel_OC	0.645
Vel_OD	0.594	Vel_OD	0.677	Vel_OD	0.650
Vel_OE	0.684	**Vel_OE**	**0.686**	Vel_OE	0.660
Vel_OU	0.520	Vel_OU	0.665	Vel_OU	0.642
Vel_S	0.694	Vel_S	0.597	Vel_S	0.634

CHAPTER 4

CONCLUSIONS

STANDING TREE ACOUSTICS

Comparison of acoustic velocities measured using transmitting and receiving probes placed on the same-face and opposite-faces for 100 standing loblolly pine (*Pinus taeda*) trees, showed significant differences in velocity between the two methods. Velocity determined using the opposite-face method generally depending on stem size, or the amount of wood through which the stress wave must pass. For the opposite-face method five possible flight paths were examined and the only opposite face method whose velocities did not vary with diameter at breast height was for an assumed flight path where the stress wave traveled from the transmitting probe around the circumference of the stem in the outerwood and then down longitudinally to the receiving probe. Variation in velocities from hit-to-hit was 62% less using the opposite-face method compared to the same-face method.

STANDING TO FELLED TREE ACOUSTICS

It was our hope was that one particular standing tree TreeSonic velocity calculation method would stand out from the rest in correlating best with the felled log HM200 velocity. If this had occurred, this might have given us insight as to which TreeSonic velocity might be the "true" velocity, or at least the one that best predicts the HM200. This was not the case. We did find that HM200 velocity tends to increase in age, as does TreeSonic velocity, and presumably stiffness.

While findings were inconclusive, however, for the 79 trees examined, the Vel_OE flight path best predicted felled tree HM200 acoustics. Further we observed that any OFM has a lower variance than the SFM (which agrees with our findings in Chapter 1). From this, we can conclude that when modeling or correlating standing tree acoustics to felled tree acoustics, the OFM is preferred.

REFERENCES

Andrews, M. 2000. Where are we with sonics? In: Workshop 2000. Capturing the Benefits of forestry Research: Putting Ideas to Work. Wood Technology Research Centre, University of Canterbury pp. 57-61.

Andrews, M. 2002. Wood quality measurement – son et lumiere. N. Z. J. For. 47:19-21.

Booker, R., and Ridoutt, B.G. 1997. Stiffness testing of standing trees. FRI Bulletin 202.

Borders, B.E., Will, R.E., Markewitz, D., Clark III, A., Hendrick, R., Teskey, R.O., and Zhang, Y. 2004. Effect of complete competition control and annual fertilization on stem growth and canopy relations for a chronosequence of loblolly pine plantations in the lower coastal plain of Georgia. For. Ecol. Manage. 192:21-37.

Briggs, D.G., and Smith, W.R. 1986. Effects of silvicultural practices on wood properties of conifers – A review. In Douglas-fir: Stand management for the future, C. Oliver, D. Hanley, and J. Johnson, eds. Seattle: Univ. of Washington Press.

Bucur, V. 2006. Acoustics of Wood, 2nd edn. Springer-Verlag, Berlin Heidelberg New York.

Carter, P., Briggs, D., Ross, R.J., and Wang, X. 2005a. Acoustic testing to enhance western forest values and meet customer wood quality needs Productivity of western forests: a forest products focus. Portland, OR : U.S. Dept. of Agriculture, Forest Service, Pacific Northwest Research Station. General technical report PNW ; GTR-642.

Carter, P., Ross, R., and Wang, X. 2005b. Characterizing Softwood Lumber Prior to Processing: New Tools and Results. 59th Forest Products Society International Convention, Québec City, Québec, Canada, 19-22 June, 2005.

Carter, P., Wang, X., Ross, R.J., and Briggs, D. 2005c. NDE of logs and standing trees using new acoustic tools – Technical application and result. Proceedings of the 14th International Symposium on Nondestructive Testing of Wood, May 2-4, 2005, University of Applied Sciences, Eberswalde, Germany. Aachen, Germany : Shaker Verlag, 2005. p.161- 169.

Chauhan, S.S., Entwistle, K.M., and Walker, J.C.F. 2005. Differences in acoustic velocity by resonance and transit-time methods in an anisotropic laminated wood medium. Holzforschung 59:428-434.

Chauhan, S.S., and Walker, J.C.F. 2006. Variations in acoustic velocity and density with age, and their interrelationships in radiata pine. For. Ecol. Manage. 229:388-394.

Clark III, A., and Daniels R.F. 2002. Modeling the effect of physiographic region on wood properties of planted loblolly pine in southeastern United States. Fourth workshop, IUFRO. S5.01.045. Harrison Hot Springs, B.C., CA. Sept 8-14.

Clark III, A., Borders, B.E., and Daniels R.F. 2004. Impact of vegetation control and annual fertilization on properties of loblolly pine wood at age 12. For. Prod. J. 54(12):90-96.

Dickson, R.L., and Matheson, A.C. 1999. Management intervention points to improve the wood quality of current and future crops. Emerging Technologies for Evaluating Wood Quality for Processing. Forest Industry Engineering Association, Melbourne 2nd December 1999.

Dickson, R.L., Joe, B., Johnston, D., Notaras, S., Notaras, B., Austin, S., Ribton-Turner, F., and Harris, P. 2004. Pre-processing prediction of wood quality in peeler logs and saw logs. In: Proceedings of the Wood Quality Conference, Albury, NSW, Australia, August.

Fox, T.R., Jokela, E.J., and Allen, H.L. 2004. The evolution of pine plantation silviculture in the Southeastern United States. Gen. Tech. Rep. SRS 75. Ashville, NC: U.S. Dept of Ag., Forest Service, Southern Research Station. 19pp.

Gorman, T.M., Wagner, F.G., and Wu, S.Y., 2003. Assessment of intensive stress-wave scanning of Douglas-fir trees for predicting lumber modulus of elasticity. In: Beall, F.C. (Ed.), Proceedings of the 13th International Symposium on Nondestructive Testing of Wood, August 19-21, 2002. University of California, Richmond, pp. 143-148.

Grabianowski, M. 2003. Measuring acoustic properties in lumber and trees. MSc Thesis, University of Canterbury, Christchurch, New Zealand.

Grabianowski, M., Manley, B., and Walker, J.C.F. 2006. Acoustic measurements on standing trees, logs, and green lumber. Wood Sci. Technol. 40:205-216.

Haygreen, J.G, and Bower, J.L. 1996. Forest products and wood science: an introduction. Third edition. Iowa State University Press. Ames, Iowa.

Hsu, C.Y. 2004. Radiata pine wood anatomy structure and biophysical properties. PhD Dissertation, University of Canterbury, Christchurch, New Zealand.

Joe, B., Dickson, R., Raymond, C., Ilic, J., and Matheson, C. 2004. Prediction of *Eucalyptus dunnii* and *Pinus radiata* timber stiffness using acoustics. RIRDC Publication No. 04/013.

Jordan, L., Clark III, A., Schimleck, L., Hall, D., and Daniels, R.F. 2007. Regional variation in wood specific gravity of plantation grown loblolly pine in the United States. Can. J. For. Res., *in press.*

Larson, P.R. 1969. Wood Formation and the Concept of Wood Quality. Bulletin No. 74. Yale University, School of Forestry.

Lasserre, J.P., Mason, E.G., and Watt, W.S. 2007. Assessing corewood acoustic velocity and modulus of elasticity with two impact based instruments in 11-year-old trees from a clonal-spacing experiment of *Pinus radiata* D. Don. For. Ecol. Manage. 239:217-221.

Lindstrom, H., Harris, P., and Nakada, R. 2002. Methods for measuring stiffness of young trees. Holz Roh Werkst. 60:165-174.

Matheson, A.C., Dickson, R.L., Spencer, D.J., Joe, B., and Ilic, J. 2002. Acoustic segregation of *Pinus radiata* logs according to stiffness. Ann. For. Sci. 59:471-477.

McKeand, S., Mullin, T., Byram T., and White T. 2003. Deployment of genetically improved loblolly and slash pine in the south. J. For. 100(3):32-37.

Neale, D.B., Sewell M.M., and Brown G.R. 2002. Molecular dissection of the quantitative inheritance of wood property traits in loblolly pine. Ann. For. Sci. 59:595-605.

Ross, R.J., Willits, S.W., Segen, W.V., Black, T., Bradshaw, B.K., and Pellerin, R.F. 1999. A stress wave based approach to NDE of logs for assessing potential veneer quality. Part I. Small-diameter ponderosa pine. For. Prod. J. 49(11):60-62.

Ross, R.R., and Pellegrin, R.F. 2004. Nondestructive testing for assessing wood members in structures: a review. General technical report FPL-GTR-70. Forest Products Laboratory. US Forest Service.

SAS Institute Inc. SAS 9.1.3 Help and documentation. Cary, NC: SAS Institute Inc., 2000-2004.

TimberMart South. 2005. Southern Timber Market Trends: August 2005. Frank W. Norris Foundation.

Toulmin, M.J., and Raymond, C.A. 2007. Developing a sampling strategy for measuring acoustic velocity in standing *Pinus radiata* using the treetap time of flight tool. N. Z. J. For. Sci. 37(1):96-111.

Wang, X., Carter, P., Ross, R.J., and Brashaw, B.K. 2007. Acoustic assessment of wood quality of raw forest materials – A path to increased profitability. For. Prod. J. 57(5):6-14.

Wang, X., Ross, R.J., and Carter, P. 2007. Acoustic evaluation of wood quality in standing trees. Part I. Acoustic wave behavior. J. Wood and Fiber Sci. 39(1):28-38.

Wang, X., Ross, R.J., Green, D.W., Brashaw, B.K., Englund, K., and Wolcott, M. 2004. Stress wave sorting for red maple logs for structural quality. Wood Sci. Technol. 37:531-537.

Wang, X., Ross, R.J., Mattson, J.A., Erickson, J.R., Forsman, J.W., Geske, E.A., and Wehr, M.A. 2002. Nondestructive evaluation techniques for assessing modulus of elasticity and stiffness of small-diameter logs. For. Prod. J. 52:79-85.

Wang, X., Ross, R.J., McClellan, M., Barbour, R.J., Erickson, J.R., Forsman, J.W., and McGinnis, G.D. 2001. Nondestructive evaluation of standing trees with a stress wave method. J. Wood and Fiber Sci. 33(4):522-533.

Wear, D.N. and J.G. Greis. 2002. Southern forest resource assessment: summary of findings. J. For. 100(7):6-14.